



TRIUMF

CANADA'S NATIONAL LABORATORY FOR PARTICLE AND NUCLEAR PHYSICS

Owned and operated as a joint venture by a consortium of Canadian universities via a contribution through the National Research Council Canada

50 Years of Cyclotrons Designed Using CYCLOPS

Y.-N. Rao, R. Baartman TRIUMF

FFAG'13, Sept.21-24, 2013

- Origins of CYCLOPS
- CYCLOPS for TRIUMF Cyclotron
- CYCLOPS for FFAG's
- Conclusions

LABORATOIRE NATIONAL CANADIEN POUR LA RECHERCHE EN PHYSIQUE NUCLÉAIRE ET EN PHYSIQUE DES PARTICULES

Propriété d'un consortium d'universités canadiennes, géré en co-entreprise à partir d'une contribution administrée par le Conseil national de recherches Canada



Where are the origins of CYCLOPS?

HIGH-ORDER DESCRIPTION OF THE DYNAMICS IN FFAGs AND RELATED ACCELERATORS

KYOKO MAKINO,* MARTIN BERZ,† PAVEL SNOPOK‡ and CAROL JOHNSTONE§

*Department of Physics and Astronomy, Michigan State University,
Fermi National Accelerator Laboratory, USA*

Department of Physics and Astronomy, University of California Riverside, USA

**makino@msu.edu*

†*berz@msu.edu*

‡*sнопok@gmail.com*

§*cjj@fnal.gov*

In this paper, we describe newly developed tools for the study and analysis of the dynamics in FFAG accelerators based on transfer map methods unique to the code COSY INFINITY. With these new tools, closed orbits, transverse amplitude dependencies and dynamic aperture are determined inclusive of full nonlinear fields and kinematics to arbitrary order. The dynamics are studied at discrete energies, via a high-order energy-dependent transfer map.

The order-dependent convergence in the calculated maps allows precise determination of dynamic aperture and detailed particle dynamics. Using normal form methods, and minimal impact symplectic tracking, amplitude- and energy-dependent tune shifts and resonance strengths are extracted. Optimization by constrained global optimization methods further refine and promote robust machine attributes.

Various methods of describing the fields will be presented, including representation of fields in radius-dependent Fourier modes, which include complex magnet edge contours and superimposed fringe fields, as well as the capability to interject calculated or measured field data from a magnet design code or actual components, respectively.

Keywords: FFAG; differential algebra; COSY INFINITY; dynamic aperture; symplectic tracking.

PACS numbers: 29.20.D-, 29.20.dg, 29.27.Bd, 87.56.bd, 41.85.Lc, 41.75.Lx, 41.75.-i

1. Introduction

The broad class of FFAG-type accelerators is experiencing an international revival in the quest for high beam power, duty cycle, reliability and, in the case of the spiral-sector FFAG, the potential for compactness at reasonable cost.^{1,2,3,4,5} The FFAGs proposed have the high average current and duty cycle characteristic of the cyclotron combined with the smaller aperture, losses, and energy variability of the synchrotron. Although new accelerator prototypes are often simulated with conventional tracking codes, these codes do not provide much flexibility in the field

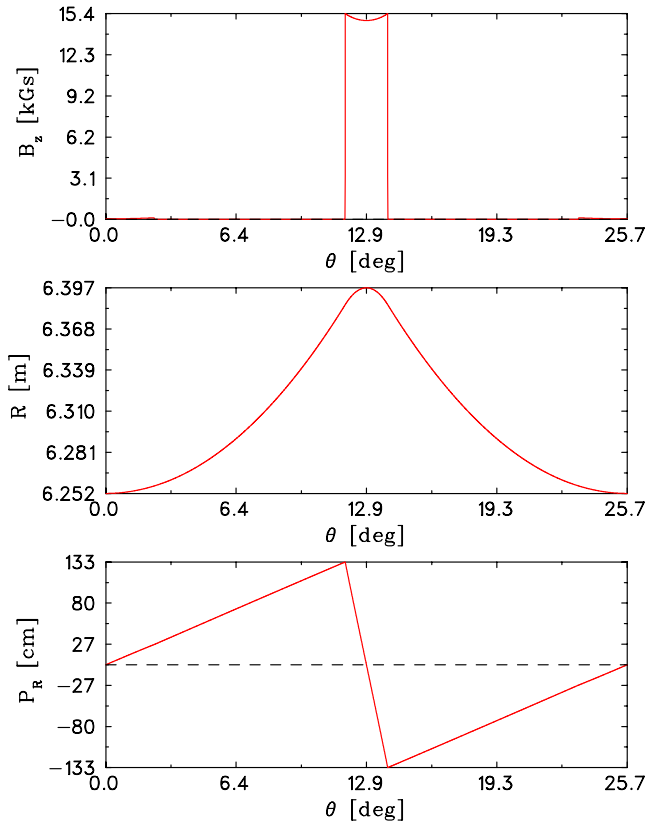



Fig. 1. B_z (vertical) field at injection for nonscaling FFAG lattice showing sharp cutoff of field at end of CF magnet, along with the radius of the injected orbit along the periodic cell and the angle as measured with respect to a normal projection relative to a radial line.

description and are limited to low order in the dynamics. This limitation can be inadequate to fully demonstrate performance including dynamic aperture where strong nonlinearities due to edge fields and other high-order effects appear. This is particularly true for the FFAGs. In the muon FFAGs, for example, the large beam emittances require the inclusion of kinematical (or angle) effects in the Hamiltonian, which implies that codes which fully describe the kinematics are necessary.^{6,7}

The current number of supported design and optimization codes that can adequately describe the complex field and magnet contours for both the scaling and nonscaling FFAG variants is limited. Outside of COSY, present public codes include only the **cyclotron code CYCLOPS**,⁸ and the field-map code ZGOUBI.^{9,10} The former, which utilizes fields and their geometry expanded in polar coordinates, has limited accuracy in this application primarily due to lack of out-of-plane expansion order, and in handling of edge-field effects; this is particularly true for the case of rapid azimuthal field fall off at magnet edges (as in the FFAG field profile of Fig. 1), an effect not present in cyclotrons. The results and derived performance

References

1. Chris Prior (Ed.). ICFA beam dynamics newsletter. Technical report, 2007.
2. M. K. Craddock. New concepts in FFAG design for secondary beam facilities and other applications. In *Proceedings, PAC05*, page 261, 2005.
3. Y. Mori. *Proceedings, FFAG05 Workshop*. FNAL, 2005.
4. K.R. Symon, D.W. Kerst, L.W. Jones, L.J. Laslett, and K.M. Terwilliger. Fixed-field alternating-gradient particle accelerators. *Physical Review*, 103:1837–1859, 1956.
5. Carol Johnstone and S. Koscielniak. *DPB Newsletter*, chapter The New Generation of FFAG Accelerators, pages 12–14. American Physical Society, 2008.
6. K. Makino and M. Berz. Effects of kinematic correction on the dynamics in muon rings. *AIP CP*, 530:217–227, 2000.
7. M. Berz, B. Erdélyi, and K. Makino. Fringe field effects in small rings of large acceptance. *Physical Review ST-AB*, 3:124001, 2000.
8. R Baartman et al. CYCLOPS. Technical report. 
9. F. Meot. The ray-tracing code ZGOUBI. *Nuclear Instruments and Methods A*, 427:353–356, 1999.
10. F. Lemuet and F. Meot. Developments in the ray-tracing code ZGOUBI for 6-d multiturn tracking in FFAG rings, 2005.
11. T. Yokoi. Private communication.
12. M. Berz. *Modern Map Methods in Particle Beam Physics*. Academic Press, San Diego, 1999. Also available at <http://bt.pa.msu.edu/pub>.
13. M. Berz. Differential algebraic description of beam dynamics to very high orders. *Particle Accelerators*, 24:109, 1989.
14. M. Berz and K. Makino. COSY INFINITY Version 9.0 beam physics manual. Technical Report MSUHEP-060804, Department of Physics and Astronomy, Michigan State University, East Lansing, MI 48824, 2006. See also <http://cosyinfinity.org>.
15. M. Berz and K. Makino. COSY INFINITY Version 9.0 programmer's manual. Technical Report MSUHEP-060803, Department of Physics and Astronomy, Michigan State University, East Lansing, MI 48824, 2006. See also <http://cosyinfinity.org>.
16. M. Tawarmalani and N. Sahinidis. *Convexification and Global Optimization and Continuous and Mixed-Integer Programming*. Kluwer, 2002.
17. C. Floudas. *Nonlinear and Mixed-Integer Optimization*. Oxford University Press, 1995.
18. K. Lange. *Optimization*. Springer, 2004.
19. M. Berz, K. Makino, and Y.-K. Kim. Long-term stability of the Tevatron by validated global optimization. *Nuclear Instruments and Methods*, 558:1–10, 2005.
20. A. Poklonskiy. *Evolutionary Optimization Methods for Beam Physics*. PhD thesis, Michigan State University, East Lansing, Michigan, USA, 2008.
21. D. W. Kerst, E. A. Day, H. J. Hausman, R. O. Haxby, L. J. Laslett, F. E. Mills, T. Ohkawa, F. L. Peterson, E. M. Rowe, A. M. Sessler, J. N. Snyder, and W. A. Wallenmeyer. Electron model of a spiral sector accelerator. *Review of Scientific Instruments*, 31,10:1076–1106, 1960.
22. E. A. Crosbie. Use of the MURA transformation to generate the fields and calculate the motion of protons in the designed Argonne mini-aspun FFAG spiral sector accelerator. *IEEE Transactions on Nuclear Science*, NS-32, 5:2675–2677, 1985.
23. K. Makino. *Rigorous Analysis of Nonlinear Motion in Particle Accelerators*. PhD thesis, Michigan State University, East Lansing, Michigan, USA, 1998. Also MSUCL-1093.
24. S. L. Manikonda and M. Berz. Multipole expansion solution of the Laplace equation using surface data. *Nuclear Instruments and Methods*, 558,1:175–183, 2006.

ADVANCES IN NONLINEAR NON-SCALING FFAGs

C. JOHNSTONE

Fermilab, Batavia, IL 60510, USA
cjj@fnal.gov

M. BERZ and K. MAKINO

Michigan State University, East Lansing, MI 48824, USA

S. KOSCIELNIAK

TRIUMF, Vancouver, BC 60439, Canada

P. SNOPOK

Illinois Institute of Technology, Chicago, IL 60616, USA

Accelerators are playing increasingly important roles in basic science, technology, and medicine. Ultra high-intensity and high-energy (GeV) proton drivers are a critical technology for accelerator-driven sub-critical reactors (ADS) and many HEP programs (Muon Collider) but remain particularly challenging, encountering duty cycle and space-charge limits in the synchrotron and machine size concerns in the weaker-focusing cyclotrons; a 10–20 MW proton driver is not presently considered technically achievable with conventional re-circulating accelerators. One, as-yet, unexplored re-circulating accelerator, the Fixed-field Alternating Gradient or FFAG, is an attractive alternative to the other approaches to a high-power beam source. Its strong focusing optics can mitigate space charge effects and achieve higher bunch charges than are possible in a cyclotron, and a recent innovation in design has coupled stable tunes with isochronous orbits, making the FFAG capable of fixed-frequency, CW acceleration, as in the classical cyclotron but beyond their energy reach, well into the relativistic regime. This new concept has been advanced in non-scaling nonlinear FFAGs using powerful new methodologies developed for FFAG accelerator design and simulation. The machine described here has the high average current advantage and duty cycle of the cyclotron (without using broadband RF frequencies) in combination with the strong focusing, smaller losses, and energy variability that are more typical of the synchrotron. The current industrial and medical standard is a cyclotron, but a competing CW FFAG could promote a shift in this baseline. This paper reports on these new advances in FFAG accelerator technology and presents advanced modeling tools for fixed-field accelerators unique to the code COSY INFINITY.¹

1. Introduction

Accelerators are playing increasingly important roles in basic science, technology, and medicine including accelerator-driven subcritical reactors, industrial irradiation, material science, neutrino production, and provide one of the most effective

6. Design and Simulation Tools

A major prerequisite for advanced accelerator design is the existence of reliable, easy to use optimization and simulation tools. Such tools are different in nature for FFAGs than those used in other kinds of accelerators; the rapidly azimuthally varying fields entail significant fringe field effects and out-of-plane nonlinearities. Tracking of orbits for assessment of dynamic aperture needs to be carried out with careful consideration of the nonlinearities, with modern methods of symplectification to insure phase space volume conservation. Further, space charge effects inherent in the high-power operation of the devices produce very novel challenges due to the necessity to treat crosstalk with neighboring orbits. Optimization challenges are difficult since they always affect many orbits at the same time and hence need to be of a global nature.

The ability to model FFAGs—both scaling and non-scaling—with conventional codes is limited. Often new prototypes of accelerators including FFAGs are simulated with codes like MAD²⁹ and Optim³⁰ as the standard codes for modeling, but these codes do not provide much flexibility in the description of the available fields and are limited to low order. This limitation can be inadequate to fully demonstrate performance including dynamic aperture, where strong nonlinearities due to edge fields and other high-order effects appear. The significant size of the beam emittance nominally invalidates the paraxial representation (kinematical, or angle effects in the Hamiltonian are significant), which implies that codes that fully represent the kinematics are necessary.

The cyclotron code **CYCLOPS**³¹ has been used to describe the FFAG, but has limited accuracy in this application primarily due to lack of out-of-plane expansion order, which specifically impacts the ability to describe dynamic aperture especially in the case of edge effects with rapid field fall-off—a condition that appears in the FFAG but is not normally present in cyclotrons. Field expansion codes such as ZGOUBI³² can accurately track the kinematics of such machines, but they have limitations when field profiles become very complex and include significant nonlinear effects. Further, ZGOUBI requires dedicated effort and expertise in order to implement a FFAG design accurately, cannot easily deal with the large transverse emittances required, and lacks some modern analysis tools for symplectic tracking, global optimization, tune shifts and chromaticities, and resonance analysis. In particular, field map codes are difficult to use when one wants to study parameter dependencies, perform detailed study of dynamic aperture, extract advanced optical functions such as high-order resonances, or use optimization routines to study the most advantageous combination of multipole correction schemes, for example.

Modern extensions of the transfer map-based philosophy,³³ as implemented in the arbitrary order code COSY INFINITY,¹ can remedy the limitation in order and in the accuracy of the dynamics. It is particularly suitable for accurate, high-order descriptions of accelerators. Yet in their standard configuration based on pre-selected field elements like combined function magnets with edge angles, they

- Terwilliger. Fixed field alternating particle accelerators, *CERN Symposium Proceedings*, v. I, p. 366, 1956.
21. D. W. Kerst, Properties of an Intersecting-Beam Accelerating System. *CERN Symposium Proceedings*, v. I, pp. 36–39, 1956.
 22. C. Johnstone, et al., Fixed Field Circular Accelerator Designs, PAC'99, New York, p. 3068.
 23. C. Johnstone, et al., A New Non-scaling FFAG for Medical Applications, *ICFA Beam Dynamics Newsletter* No. 43, July, 2007, <http://www-bd.fnal.gov/icfabd/Newsletter43.pdf>, pp. 125–132.
 24. C. Johnstone, et al., A New Non-scaling FFAG for Medical Applications, *Proc. of the Particle Accelerator Conference*, Albuquerque, NM, p. 2951, 2007.
 25. C. Johnstone, et al., Tune-stabilized Linear Field FFAG for Carbon Therapy, *Proc. of the 2006 European Particle Accelerator Conference*, Edinburgh, UK, pp. 2290–2292, 2006.
 26. K. Makino, et al., High-order Description of the Dynamics in FFAGs and Related Accelerators, *Int. Journal of Mod. Physics-A*, vol. 24, No. 5, pp.908–22 (2009).
 27. S. Machida, *Proc. U.S. Particle Accelerator Conference PAC'07*, Albuquerque, NM, 2007.
 28. S. Smith, et al., to be published, *Proc. Cyclotrons'10*, Lanzhou, China, 2010.
 29. MAD Version 9, <http://wwwslap.cern.ch/mad/>.
 30. V. Lebedev, OptiM. <http://www-bdnew.fnal.gov/pbar/organizationalchart/lebedev/OptiM/optim.htm>.
 31. R. Baartman, et al., CYCLOPS.
 32. F. Meot, The Ray-Tracing Code Zgoubi, *Nuclear Instruments and Methods A*, v. 427, pp. 353–356. 1999.
 33. M. Berz, Modern Map Methods in Particle Beam Physics, *Academic Press*, San Diego, 1999. M. Berz, Differential Algebraic Description of Beam Dynamics to Very High Orders, *Particle Accelerators*, v. 24, p. 109, 1989.
 34. B. Erdelyi, et al., Optimal Symplectic Approximation of Hamiltonian Flows, *Phys. Rev. Lett.* 87(11) (2001) 114302. B. Erdleyi, et al., Local Theory and Applications of Extended Generating Functions, *Int. J. Pure Appl. Math.* 11(3) (2004) 241-282.
 35. M. Craddock, et al., to be published, *Proc. Cyclotrons'10*, Lanzhou, China, 2010.

COMPUTATION OF CLOSED ORBITS AND BASIC FOCUSING PROPERTIES FOR SECTOR-FOCUSED CYCLOTRONS AND THE DESIGN OF “CYCLOPS”[†]

M. M. GORDON

National Superconducting Cyclotron Laboratory
Michigan State University
East Lansing, MI 48824

(Received November 7, 1983)

The program Cyclops, like the Equilibrium Orbit Code before it, calculates with optimum efficiency all the important properties of the closed orbits and of the linear radial and vertical oscillations about these orbits. Such orbits include both normal equilibrium orbits and those displaced by field perturbations, as well as unstable fixed-point orbits associated with certain nonlinear resonances. Given the median-plane magnetic field in polar coordinates, the program uses direct numerical integration of the canonical equations of motion (together with special iteration and extrapolation procedures for obtaining the correct initial conditions) to calculate these orbit properties as a function of the ion energy over the range available in the given field. At each energy, the output provides values of the focusing frequencies, eigenellipse parameters, and form factors for the linear oscillations, as well as data on the frequency error and phase slip. A reasonably detailed discussion is presented of the theoretical basis for these calculations, along with some applications of the results to the design and analysis of sector-focused cyclotrons.

1. INTRODUCTION

Ever since its early development at Oak Ridge,¹ the Equilibrium Orbit Code has been one of the most-useful computer programs available to those engaged in the design and analysis of sector-focused cyclotrons. Given the median-plane field $B(r, \theta)$ in polar coordinates, this program computes at each energy all the important properties of the equilibrium orbit (EO) and of the linear radial and vertical oscillations about this orbit. These include, of course, the orbit period τ and the focusing frequencies ν_r and ν_z .

The EO Code is based on direct numerical integration of the canonical equations of motion, and the key element of this program is the efficient iteration scheme by which it determines the EO coordinates r and p_r as a function of θ . Such a scheme is practically essential, since for sector-focused cyclotrons with isochronous fields, the shape of the EO generally changes with energy and the q/m of the ion, as well as the magnet excitation.

As was discovered somewhat later, the EO Code can also be used to calculate any other closed orbit in the median plane of the given field.² Such orbits include, for

[†] Work supported by the National Science Foundation under Grant No. Phy 78-22696.

example, the unstable fixed-point orbits associated with $\nu_r = N/3$ or $N/4$ nonlinear resonance. In such cases, the program produces data showing the variation of the stability limits with energy, and thereby assists in the construction of radial phase-space diagrams. Recent examples of these applications are shown in Figs. 1 and 2.

Moreover, when imperfections are added to the median-plane field, the same iteration scheme enables the program to locate the displaced *EO*'s or other fixed-point orbits. At the same time, the program provides values of ν_r and ν_z for the displaced orbits, and this information helps in evaluating possible resonance effects produced by the given field imperfections. See, for example, Fig. 2.

One should, of course, keep in mind that the results of analytical treatments of most (but not all) of these phenomena have long been available through the work of Smith and Garren,³ Parzen,⁴ and especially Hagedoorn and Verster.⁵ These analytical results are most useful in revealing how various orbit properties depend on specific parameters of the magnetic field. However, when highly accurate results are required on a routine basis, then the *EO* Code becomes practically indispensable.

The first Fortran version of this program was completed in 1964 and named *Cyclops*, short for *Cyclotron Closed Orbit Program*.⁶ Not long thereafter, a modified version was developed by Joho⁷ in connection with the design of the large SIN Cyclotron. Later, the original *Cyclops* program was transferred to Vancouver, where it was adapted by Mackenzie, Kost, and coworkers for design work on the large TRIUMF cyclotron.⁸ In particular, this group developed an extended version of *Cyclops* in order to generate the data required for a transfer-matrix program ("COMA") which very efficiently calculates large groups of accelerated orbits assuming linear, but non-adiabatic conditions.⁹ More recently, the TRIUMF group has employed *Cyclops* in their design work on high-energy cyclotrons for possible use as "kaon factories."¹⁰

The main reason for writing this report now is that we are planning a new version of the *Cyclops* program that will incorporate all the improvements suggested by twenty years of experience here and elsewhere. Our aim, therefore, is to present a reasonably complete discussion of the theoretical basis for this program in order to make its construction and operation sufficiently clear to those who might be interested in using or writing such a program. Moreover, much of the material presented here is not generally available elsewhere.

The *Cyclops* program differs from the original *EO* Code mainly in the amount of information it provides on the linear oscillations. That is, the *EO* Code gives only the values of ν_r and ν_z , while *Cyclops* provides, in addition, such quantities as $\alpha(\theta)$ and $\beta(\theta)$, the well-known parameters characterizing the periodic transfer matrix.¹¹ As in synchrotron applications, these parameters can be used to find the eigenellipse properties as well as the width functions and form factors for the radial and vertical oscillations.

However, the definition and interpretation of $\alpha(\theta)$ and $\beta(\theta)$ are somewhat different from those usually found in synchrotron work. This difference results mainly from our formulation of the equations of motion, and because of this difference, we present here a somewhat more detailed discussion of the theory than would otherwise be necessary.

We should note, in particular, that because we use canonical variables, the resultant width functions automatically contain the adiabatic damping. That is, our β varies as R/p , and this form seems much more appropriate for isochronous cyclotrons where R and p increase rapidly with energy, but the ratio R/p does not.

After the output has been inspected, it may seem desirable to modify the frequency ω_0 and it should be emphasized that such a change can be made quite easily without rerunning the program. That is, if a fractional shift ϵ' is made in the frequency, as defined by

$$\omega_0' = (1 + \epsilon')\omega_0, \quad (70)$$

then from the definition (66), the revised frequency error becomes

$$\Omega'(E) = (1 + \epsilon')\Omega(E) + \epsilon'. \quad (71)$$

As a result of Eq. (69), we then find that $F(E) \rightarrow F'(E)$ given by

$$F'(E) = (1 + \epsilon')F(E) + 2\pi\epsilon'(E - E_i). \quad (72)$$

Thus, since ϵ' is generally very small, this change produces a nearly linear shift of the $\sin \phi$ vs E curve.

11. CONCLUDING REMARKS

Cyclotrons with radial sectors, like those at Indiana and GANIL in France, have extra magnetic symmetry and because of this, the EO 's in these machines have $p_r = 0$ at the center of each hill and valley. As a result, the calculation of normal EO and focusing properties requires orbit integration only through half a sector, i.e., from the center of a valley to the center of a hill (or vice versa). For such cases, we developed a special form of the EO Code which was then used in the final design of the Indiana cyclotron.¹⁵

It is also worth mentioning that an unusual overwrite has been incorporated into the TRIUMF version of Cyclops which enables the program to handle situations where the EO is slightly displaced from the nominal median plane as a result of magnet imperfections.¹⁶ In addition to the usual map of B_z , this version of Cyclops requires values of B_r , B_θ , and $\partial B_z/\partial z$ in the place $z = 0$. It then uses modified equations of motion, which include zero- and first-order terms in z and p_z to calculate the displaced EO and the resultant focusing properties.

Since there exist now many individual EO Codes that have been developed at various laboratories, it seems highly desirable to have some standard cyclotron magnetic field established to serve as a test case for purposes of comparison. Such a field was devised by a group at SIN and this field has the twin virtues of being analytical in form and quite realistic as well. The relevant report¹⁷ contains a listing for the subroutine that generates the field, together with a sample output.

In conclusion, I would like to express my gratitude to G. Mackenzie and his coworkers at TRIUMF for many useful discussions, and also to F. Marti and B. Milton for constructing the figures. Finally, I am most indebted to my wife Bernice, who continues to provide indispensable assistance as my reader and editor.

REFERENCES

1. M. M. Gordon and T. A. Welton, Oak Ridge National Lab., ORNL Report, 2765, (1959).
2. M. M. Gordon and W. S. Hudec, *Nucl. Instrum. Methods*, **18-19**, 243 (1962); M. M. Gordon and H. G. Blosser, *Ibid.*, 378.

ORNL-2765
Particle Accelerators and
High Voltage Machines

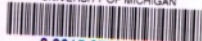
COMPUTATION METHODS FOR AVF
CYCLOTRON DESIGN STUDIES

M. M. Gordon
T. A. Welton



OAK RIDGE NATIONAL LABORATORY
operated by
UNION CARBIDE CORPORATION
for the
U.S. ATOMIC ENERGY COMMISSION

UNIVERSITY OF MICHIGAN



3 9015 07731 4667

ORNL-2765

Copy _____

Contract No. W-7405-eng-26

Physics Division

COMPUTATION METHODS FOR AVF CYCLOTRON DESIGN STUDIES

M. M. Gordon and T. A. Welton

Date Issued

SEP 11 1959

OAK RIDGE NATIONAL LABORATORY
Oak Ridge, Tennessee
Operated by
UNION CARBIDE CORPORATION
for the
U. S. ATOMIC ENERGY COMMISSION



**CYCLOPS was originated
at ORNL & MSU,
transferred to TRIUMF and
developed at TRIUMF.**



What does CYCLOPS do?

- It calculates with optimum efficiency all the important properties of the closed orbits and of the linear radial and vertical oscillations about these orbits. Such orbits include both normal equilibrium orbits and those displaced by field perturbations, as well as unstable fixed-point orbits associated with certain nonlinear resonances.
- Given the median-plane magnetic field in polar coordinates, the program uses direct **numerical integration of the canonical equations of motion** (together with special iteration and extrapolation procedures for obtaining the correct initial conditions) to calculate these orbit properties as a function of the ion energy over the range available in the given field.
- At each energy, the program output provides values of the **focusing frequencies, eigenellipse parameters**, and form factors for the linear oscillations, as well as data on the **frequency error and phase slip**.



Equations of Motion

**CYCLOPS has already built into it differential equations:
(The most convenient independent variable is azimuth θ .)**

$$\begin{aligned}\frac{dr}{d\theta} &= r \frac{p_r}{p_\theta} \\ \frac{dp_r}{d\theta} &= p_\theta - r B_z + r \frac{p_z}{p_\theta} B_\theta \\ \frac{dz}{d\theta} &= r \frac{p_z}{p_\theta} \\ \frac{dp_z}{d\theta} &= r B_r - r \frac{p_r}{p_\theta} B_\theta \\ \frac{dt}{d\theta} &= \gamma \frac{r}{p_\theta}\end{aligned}$$

**These equations
are canonical.**

where $p_\theta = \sqrt{p^2 - p_r^2 - p_z^2}$. These are in cyclotron units: B in unit of central field $m\omega_0/q$, t in unit of ω_0^{-1} , lengths in unit of c/ω_0 , p in unit of mc .



Field Map

The field components used are shown below and are correct to the 2nd order in z :

$$B_r = B_r(z = 0) + z \left(\frac{\partial B_z}{\partial r} \right) + \frac{z^2}{2} \left[\frac{\partial^2 B_z}{\partial r \partial z} \right]$$

$$B_\theta = B_\theta(z = 0) + \frac{z}{r} \left(\frac{\partial B_z}{\partial \theta} \right) + \frac{z^2}{2r} \left[\frac{\partial^2 B_z}{\partial \theta \partial z} \right]$$

$$B_z = B_z(z = 0) + z \left(\frac{\partial B_z}{\partial z} \right) - \frac{z^2}{2} (\Gamma^2 B_z)$$

$$\Gamma^2 = \frac{\partial^2}{\partial r^2} + \frac{1}{r} \frac{\partial}{\partial r} + \frac{1}{r^2} \frac{\partial^2}{\partial \theta^2}$$

where the partial derivatives are taken in the geometrical median plane where $z = 0$; also $B_r(z = 0)$, $B_\theta(z = 0)$, $B_z(z = 0)$ are meant the field components in the GMP.

**These satisfy
Maxwell's
equations.**



Iteration Procedure

We integrate over one sector of a N-sector machine. But of course the orbit will not close on itself. To find the closed orbit, we track the first order differential equations of motion as well. Let $r \longrightarrow r + x$, $p_r \longrightarrow p_r + p_x$, and keep only the first order terms, we obtain linear oscillation equations:

$$\begin{aligned}\frac{dx}{d\theta} &= \frac{p_r}{p_\theta} x + \frac{r p_\theta^2}{p_\theta^3} p_x \\ \frac{dp_x}{d\theta} &= - \left[B_z + r \frac{\partial B_z}{\partial r} \right] x - \frac{p_r}{p_\theta} p_x \\ \frac{dz}{d\theta} &= \frac{r}{p_\theta} p_z \\ \frac{dp_z}{d\theta} &= \left[r \frac{\partial B_z}{\partial r} - \frac{p_r}{p_\theta} \frac{\partial B_z}{\partial \theta} \right] z\end{aligned}$$

These are integrated with initial values: $(x, p_x) = (1, 0), (0, 1); (z, p_z) = (1, 0), (0, 1)$, and give the transfer matrix:

$$R_x = \begin{pmatrix} x_1 & x_2 \\ p_{x1} & p_{x2} \end{pmatrix}_\theta, \quad R_z = \begin{pmatrix} z_1 & z_2 \\ p_{z1} & p_{z2} \end{pmatrix}_\theta$$



Iteration Procedure — cont'd

These are used in an iteration to calculate improved trial values to find the closed orbit:

$$\begin{pmatrix} r_c \\ p_{rc} \end{pmatrix}_\theta - \begin{pmatrix} r \\ p_r \end{pmatrix}_\theta = R_x \begin{pmatrix} \delta r_i \\ \delta p_{ri} \end{pmatrix},$$

where $(\delta r_i, \delta p_{ri})$ are the corrections being sought for the initial values: $r_{ci} = r_i + \delta r_i$ and $p_{rci} = p_{ri} + \delta p_{ri}$, (r_c, p_{rc}) and (r, p_r) are the coordinates of the closed orbit and the trial orbit (computed already).

Applying this equation at initial and final azimuths and taking the difference, we obtain

$$0 = \begin{pmatrix} \epsilon_1 \\ \epsilon_2 \end{pmatrix} + (R_x - I) \begin{pmatrix} \delta r_i \\ \delta p_{ri} \end{pmatrix},$$

which then gives the corrections

$$\delta r_i = \frac{(R_{22} - 1) \epsilon_1 - R_{12} \epsilon_2}{R_{11} + R_{22} - 2},$$
$$\delta p_{ri} = \frac{(R_{11} - 1) \epsilon_2 - R_{21} \epsilon_1}{R_{11} + R_{22} - 2}.$$

where $\epsilon_1 = r - r_i$, $\epsilon_2 = p_r - p_{ri}$ are the errors in the trial values at start. The change $r_i \longrightarrow r_i + \delta r_i$, $p_{ri} \longrightarrow p_{ri} + \delta p_{ri}$, will provide improved initial values for the next cycle until $\epsilon_{1,2} < \epsilon_0$. Similar process for the z -motion.



Calculations of (ν_r, ν_z) and (α, β, γ)

Since the transfert matrix is obtained for one complete period, represented as

$$R = I \cos \mu + J \sin \mu$$

where I is unit matrix and

$$J = \begin{pmatrix} \alpha & \beta \\ -\gamma & -\alpha \end{pmatrix}.$$

Thus

$$\cos \mu = (R_{11} + R_{22})/2$$

$$\alpha \sin \mu = (R_{11} - R_{22})/2$$

$$\beta \sin \mu = R_{12}$$

$$\gamma \sin \mu = -R_{21}$$

and since $|R| = 1$, we also have

$$\beta\gamma = 1 + \alpha^2.$$

These equations determine $\sin \mu$ as well as $\cos \mu$, and calculate ν_r and ν_z

$$\nu = \frac{N \mu}{2\pi}$$

when $|\cos \mu| \leq 1$ so the motion is stable.

And then, using the similarity transformation, we obtain (α, β, γ) at any azimuth

$$\begin{pmatrix} \beta \\ \alpha \\ \gamma \end{pmatrix}_\theta = \begin{pmatrix} R_{11}^2 & -2R_{11}R_{12} & R_{12}^2 \\ -R_{11}R_{21} & R_{11}R_{22} + R_{12}R_{21} & -R_{12}R_{22} \\ R_{21}^2 & -2R_{21}R_{22} & R_{22}^2 \end{pmatrix} \begin{pmatrix} \beta \\ \alpha \\ \gamma \end{pmatrix}_i$$

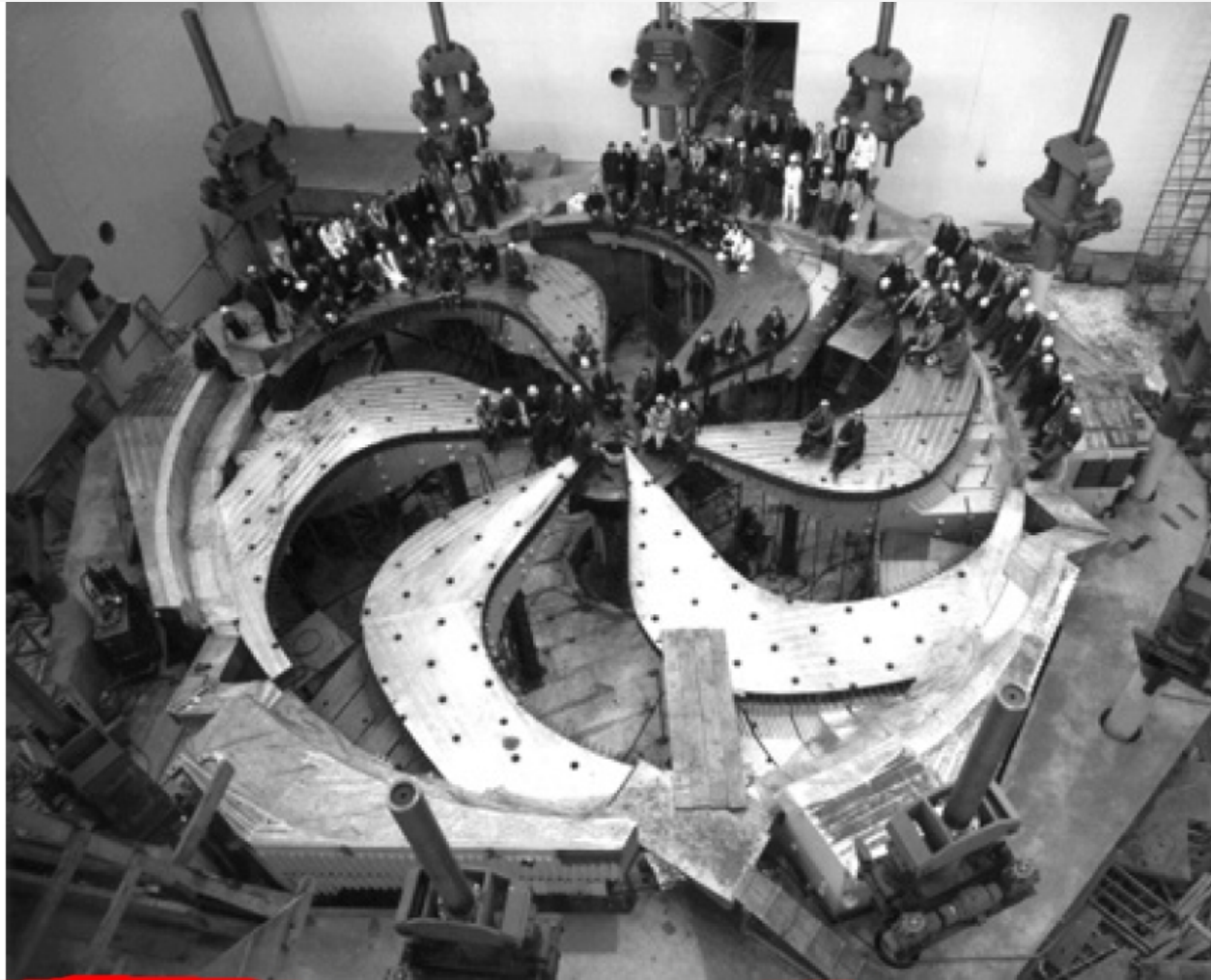


- **CYCLOPS** is NOT finding transfer matrices by taking differences of orbit coordinates from the closed orbit. Instead, it is finding transfer matrices and tunes by tracking first order differential equations.
- **CYCLOPS** is working in a sense just like COSY-Infinity, except that the map is only to the 1st order. In a sense, **CYCLOPS** is a precursor of COSY.



TRIUMF Cyclotron was designed using CYCLOPS.

Words of one of the inventors of the FFAG!



The TRIUMF FFAG spiral sector cyclotron [520 MeV H^+ ions]
at the University of British Columbia in Vancouver, Canada



TRIUMF Details

- At 500 MeV, $\langle B \rangle = 0.4632$ T, $\langle R \rangle = 308$ inches.
- RF volts per turn = 0.4 MV.
- Number of turns to 500MeV = 1250.
- RF harmonic number=5:

A field error of

$$\frac{\Delta \bar{B}}{\bar{B}} = \frac{\Delta \phi}{\Delta N 2\pi h} = \frac{180^\circ}{1250 \times 360^\circ \times 5} = \frac{1}{12,500}$$

results in a phase slip of 180° .

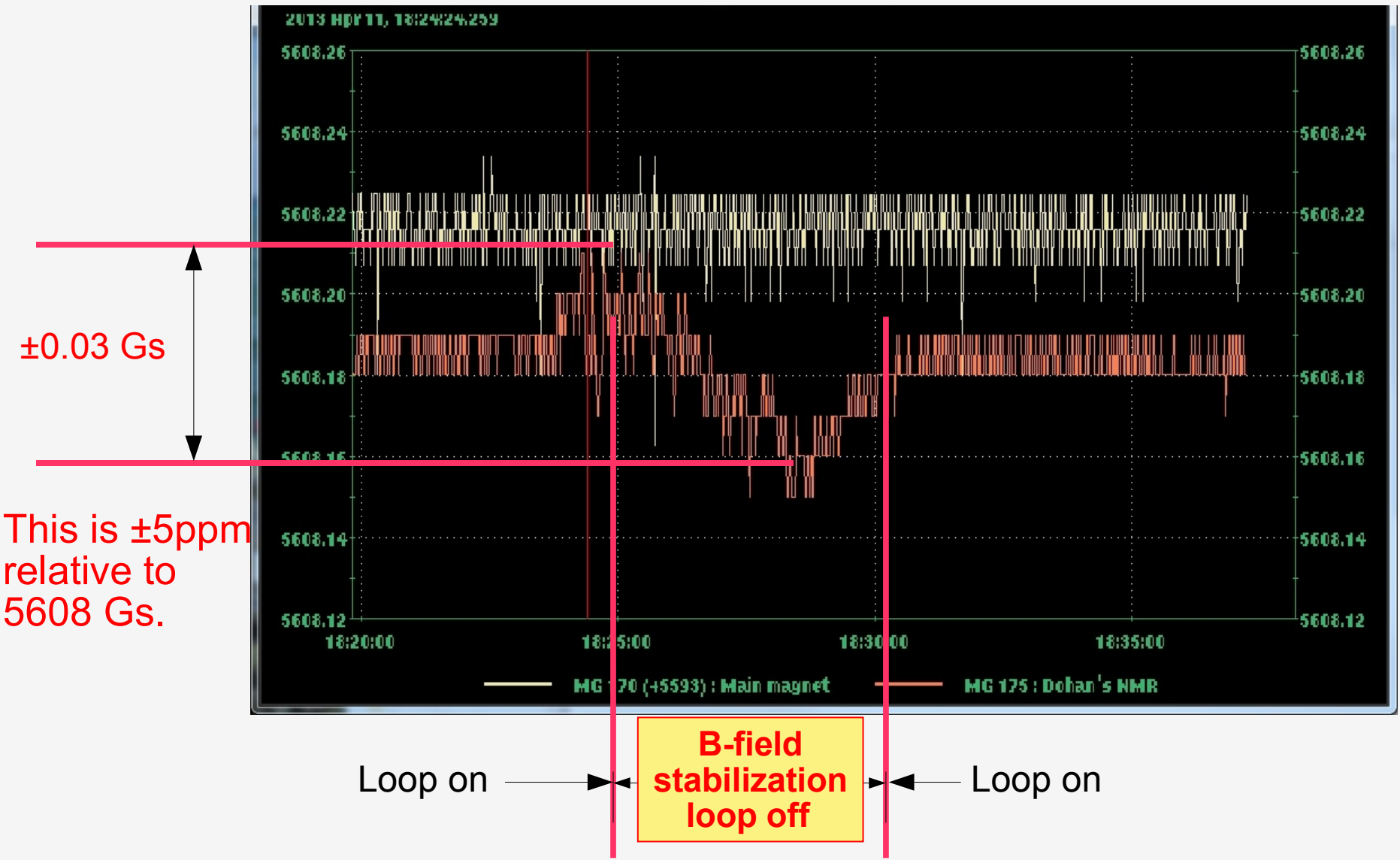
This means that the magnetic field tolerance is only 5 ppm for allowed phase wander of 10° .

This is the ACCURACY required!



TRIUMF Details

5ppm magnetic field accuracy is achieved!





TRIUMF Details

How was such an accuracy achieved?

This accuracy was achieved with a measurement system of 100 tiny flip-coils. The field was shimmed, measured, CYCLOPS'd, shimmed, measured, CYCLOPS'd, shimmed, measured, CYCLOPS'd, shimmed, measured, CYCLOPS'd, shimmed, measured, CYCLOPS'd.

It had to be within a few ppm everywhere, and then when the beam was turned on in 1974, it actually worked.



Tune Measured

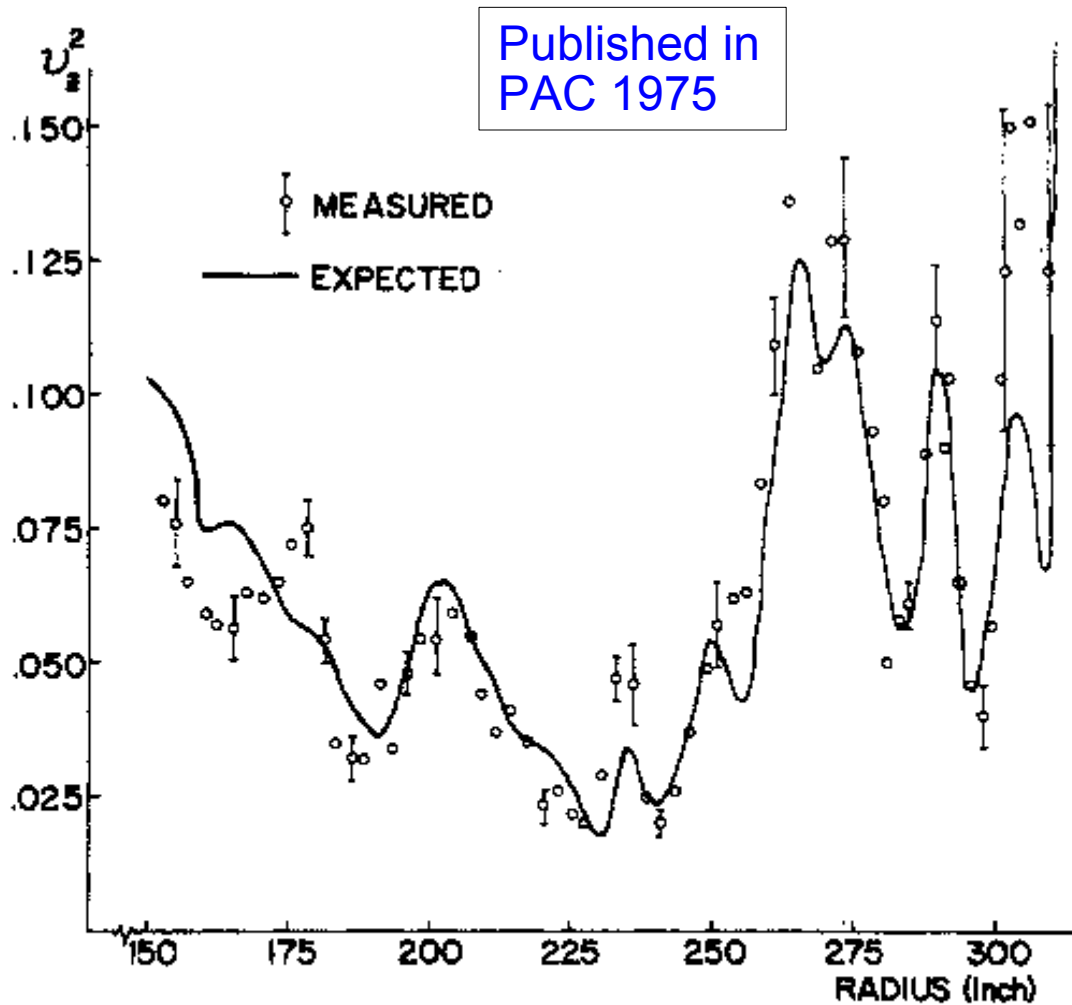


Figure 6. v_x^2 as a function of radius. The points were obtained from measurements with the beam, the curve from calculations based on a magnetic field survey.

- By measuring the change in mean height of beam for a given change in $\langle B_r \rangle$ obtained by adjusting the trim coil currents.
- The measured tune **appeared to be in reasonably good agreement with CYCLOPS calculated result.**



$\nu_r = 3/2$ Resonance

J.R. Richardson, AIP Conf. 1972

STUDIES IN BEAM DYNAMICS

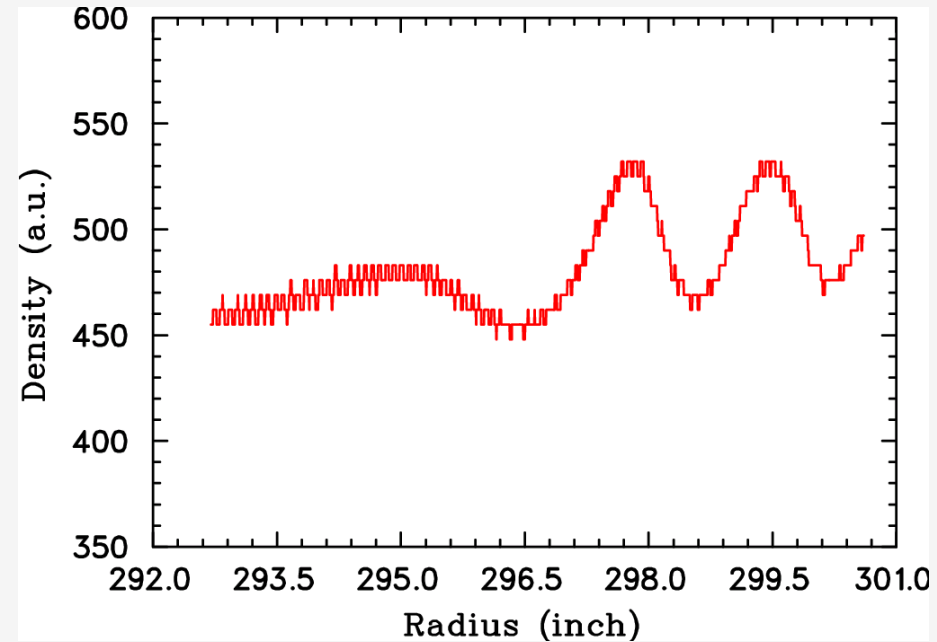
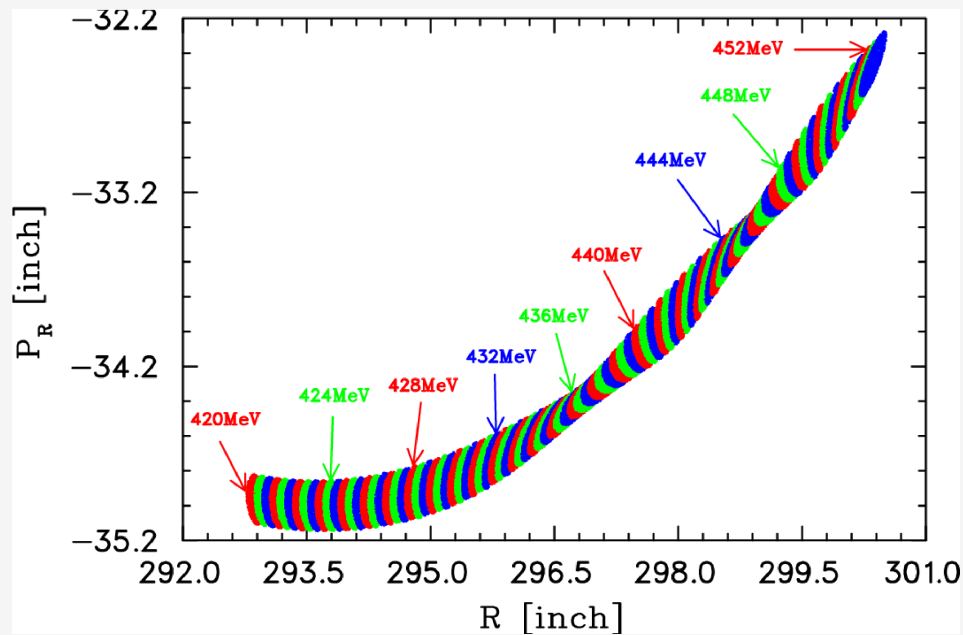
The effects of resonances on the TRIUMF beam quality have been studied.⁹ In accordance with previous discussions, it was found that TRIUMF is approximately a factor of ten more sensitive than most cyclotrons to the presence of a first harmonic in the magnetic field. Detailed orbit calculations have shown that 0.2 G first harmonic produces a serious effect on the radial amplitude, but that the effect can be reduced to a negligible value by use of the harmonic coils being installed on the vacuum chamber. It was also found that the tolerances on the first harmonic twist in the median plane due to the $\nu_x - \nu_z = 1$ resonance are not too difficult to satisfy while in the neighbourhood of the $\nu_x = 1.5$ resonance the gradient of the third harmonic must be less than 0.2 G/in.

In fact, the radial gradient of the 3rd harmonic error was reduced to ≤ 0.1 G/inch.



Simulations

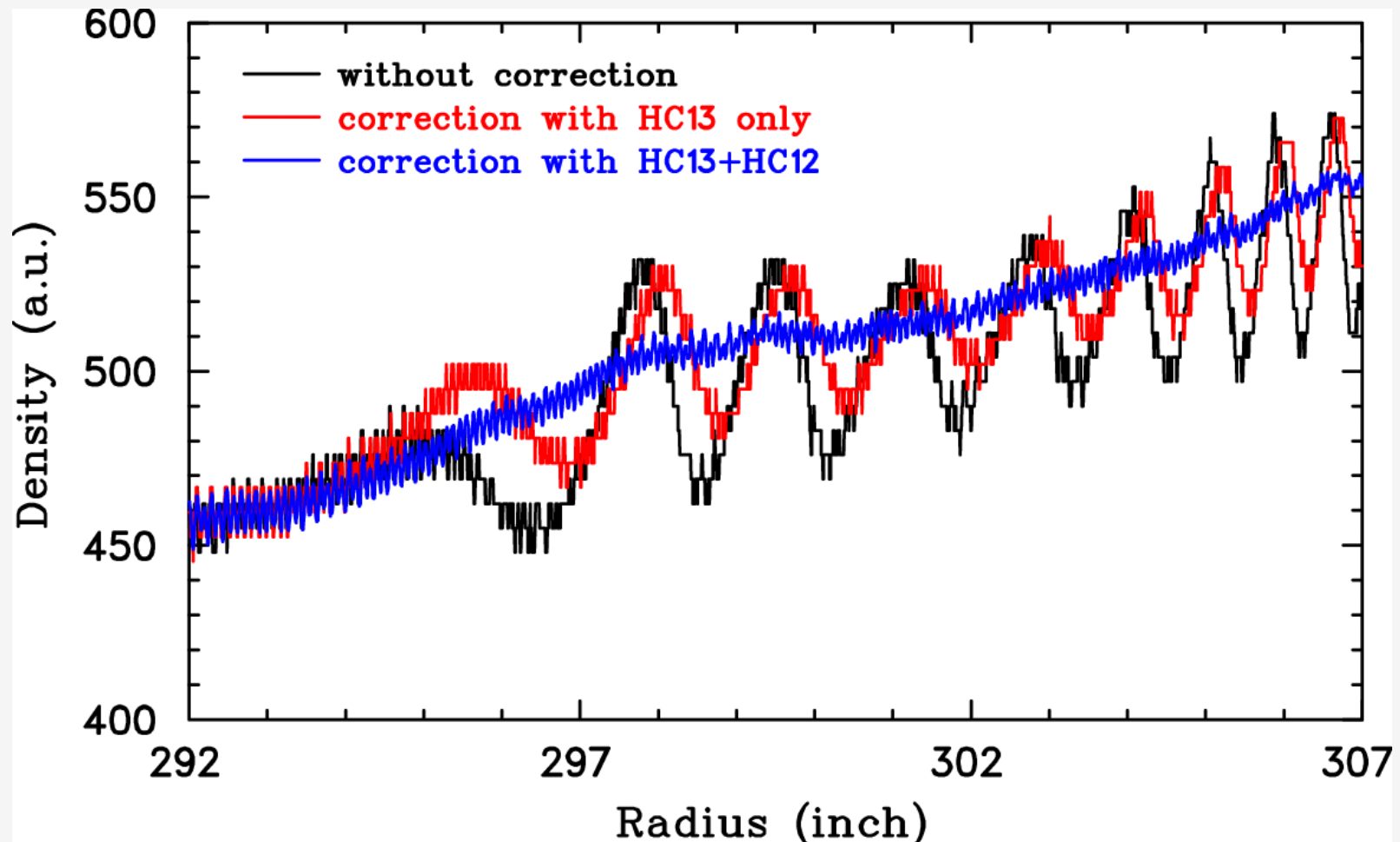
Made using **CYCLOPS** generated transfer matrices:





Corrections

Simulated result using **CYCLOPS** generated transfer matrices:

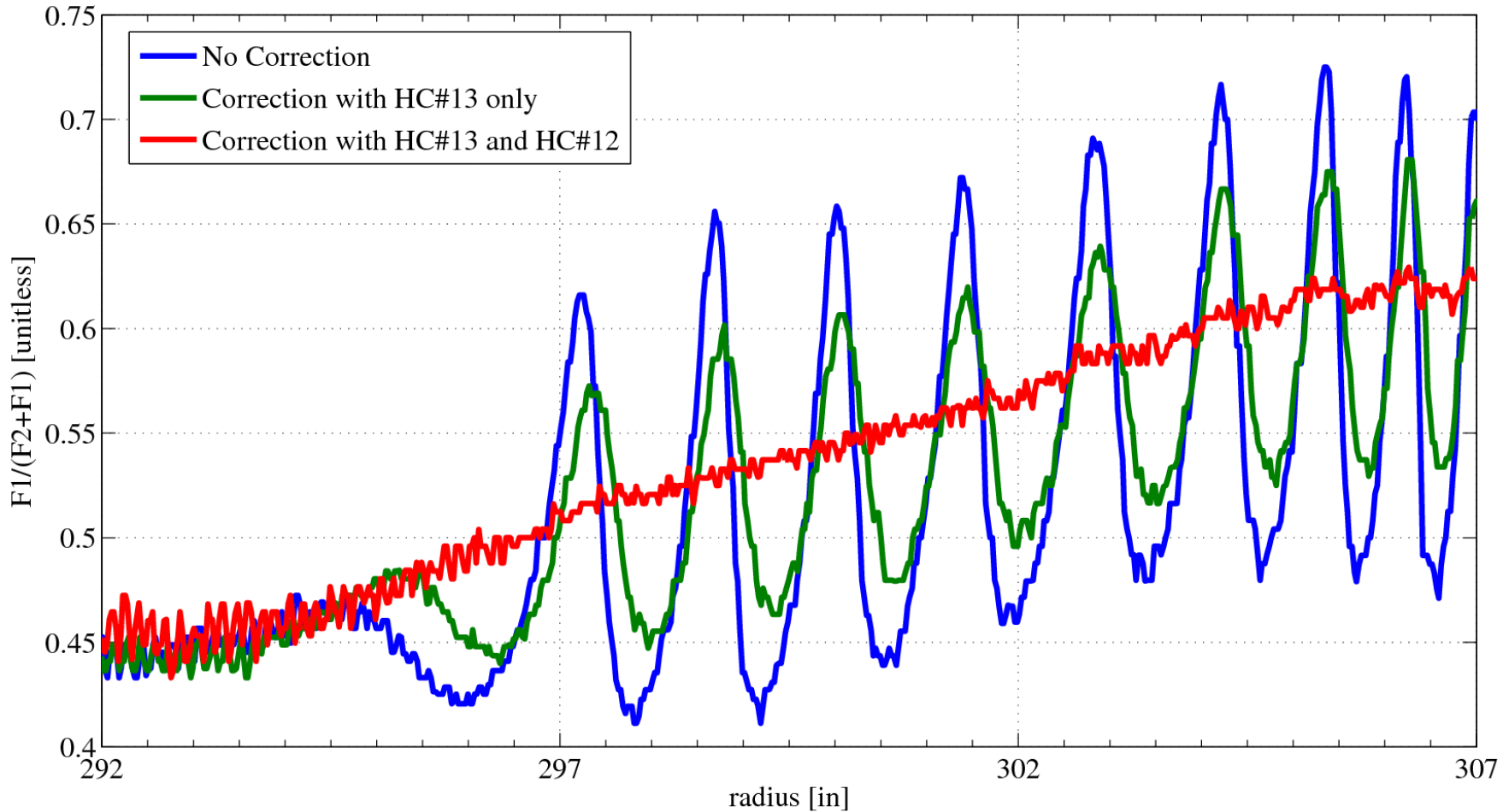




Corrections

Measured result, exactly as the simulations predicted:

HE2 probe – current density pattern



With correction, we must be reducing by 10x to ≤ 0.01 G/inch.



Also, CYCLOPS can calculate unstable fixed point orbits associated with $\nu=N/3$ or $N/4$ nonlinear resonance, thereby constructing phase space stability limits diagram.

COMPUTATION OF CLOSED ORBITS AND BASIC FOCUSING PROPERTIES FOR SECTOR-FOCUSED CYCLOTRONS AND THE DESIGN OF “CYCLOPS”[†]

M. M. GORDON

National Superconducting Cyclotron Laboratory
Michigan State University
East Lansing, MI 48824

(Received November 7, 1983)

The program Cyclops, like the Equilibrium Orbit Code before it, calculates with optimum efficiency all the important properties of the closed orbits and of the linear radial and vertical oscillations about these orbits. Such orbits include both normal equilibrium orbits and those displaced by field perturbations, as well as unstable fixed-point orbits associated with certain nonlinear resonances. Given the median-plane magnetic field in polar coordinates, the program uses direct numerical integration of the canonical equations of motion (together with special iteration and extrapolation procedures for obtaining the correct initial conditions) to calculate these orbit properties as a function of the ion energy over the range available in the given field. At each energy, the output provides values of the focusing frequencies, eigenellipse parameters, and form factors for the linear oscillations, as well as data on the frequency error and phase slip. A reasonably detailed discussion is presented of the theoretical basis for these calculations, along with some applications of the results to the design and analysis of sector-focused cyclotrons.

1. INTRODUCTION

Ever since its early development at Oak Ridge,¹ the Equilibrium Orbit Code has been one of the most-useful computer programs available to those engaged in the design and analysis of sector-focused cyclotrons. Given the median-plane field $B(r, \theta)$ in polar coordinates, this program computes at each energy all the important properties of the equilibrium orbit (*EO*) and of the linear radial and vertical oscillations about this orbit. These include, of course, the orbit period τ and the focusing frequencies ν_r and ν_z .

The *EO* Code is based on direct numerical integration of the canonical equations of motion, and the key element of this program is the efficient iteration scheme by which it determines the *EO* coordinates r and p_r as a function of θ . Such a scheme is practically essential, since for sector-focused cyclotrons with isochronous fields, the shape of the *EO* generally changes with energy and the q/m of the ion, as well as the magnet excitation.

As was discovered somewhat later, the *EO* Code can also be used to calculate any other closed orbit in the median plane of the given field.² Such orbits include, for

[†] Work supported by the National Science Foundation under Grant No. Phy 78-22696.

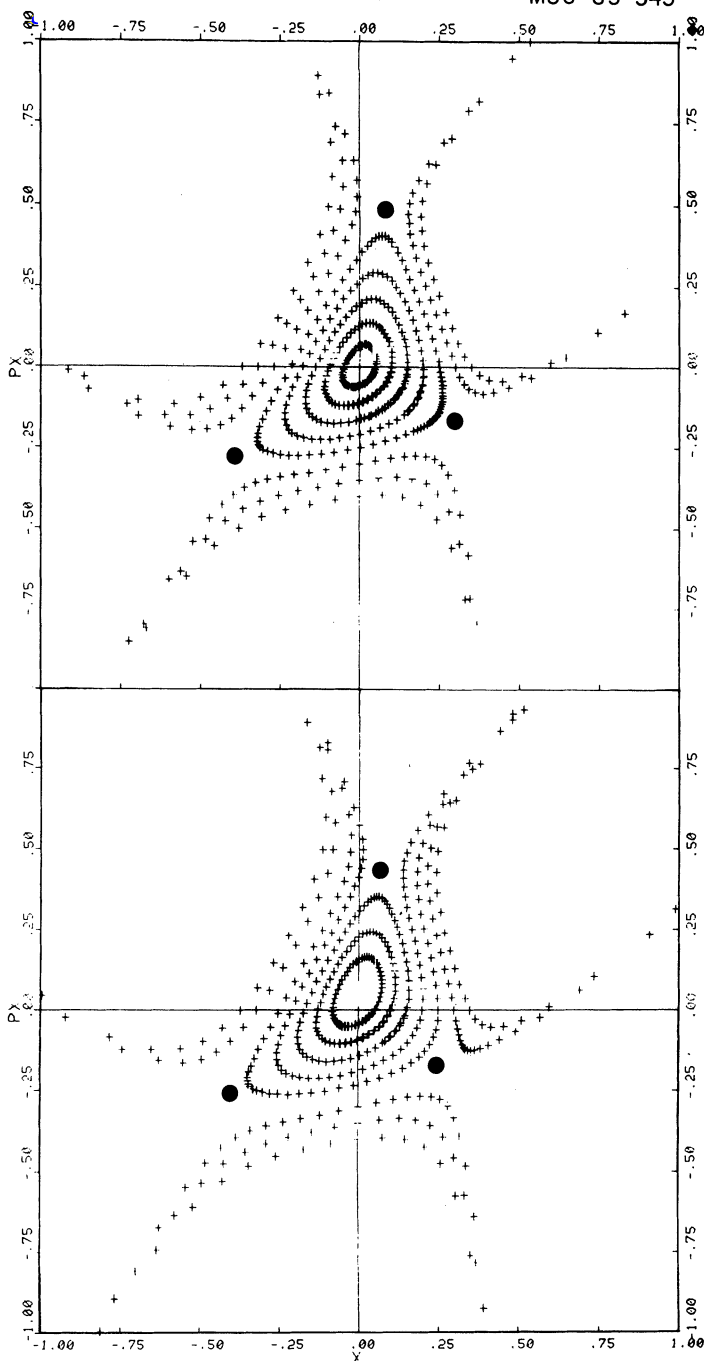


FIGURE 2 Two radial phase-space diagrams characterizing the behavior of a variety of stable and unstable orbits, all at 28 MeV/A. Each orbit is represented by a sequence of (x, p_x) points (shown as crosses) which are plotted once per turn along the same spiral curve used for Fig. 1. The data for the upper diagram were obtained with the perfect $N = 3$ field, for which $\nu_r = 1.0214$ and $\nu_z = 0.4457$ at this energy. The lower diagram was derived from the actual field and shows the changes produced by the presence of small $N' = 1$ and 2 components. In this case, $\nu_r = 1.0211$ and $\nu_z = 0.4462$ for the displaced EO. The three unstable fixed points are shown as solid circles and all have complex ν_z as well as complex ν_r values. For example, the fixed point closest to the EO in the lower diagram has $\nu_r = 1.0 + i(0.0367)$ and $\nu_z = 0.5 + i(0.0330)$. These values indicate the quantitative effects of both the $\nu_r = 3/3$ and $\nu_r = 2\nu_z$ nonlinear resonances which are evidently nearby.

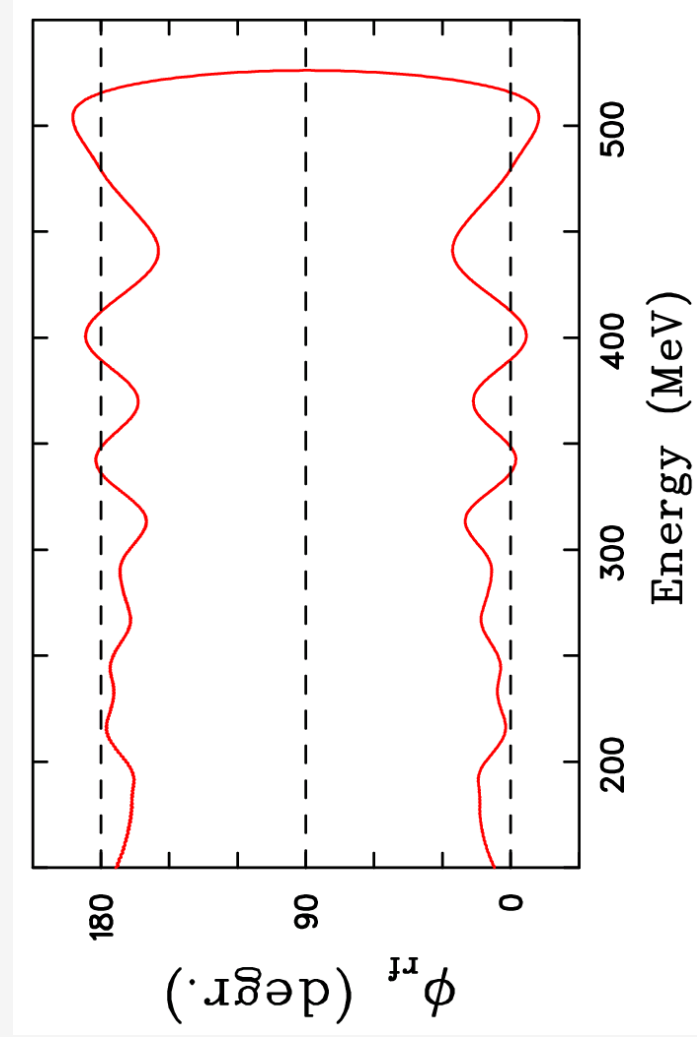
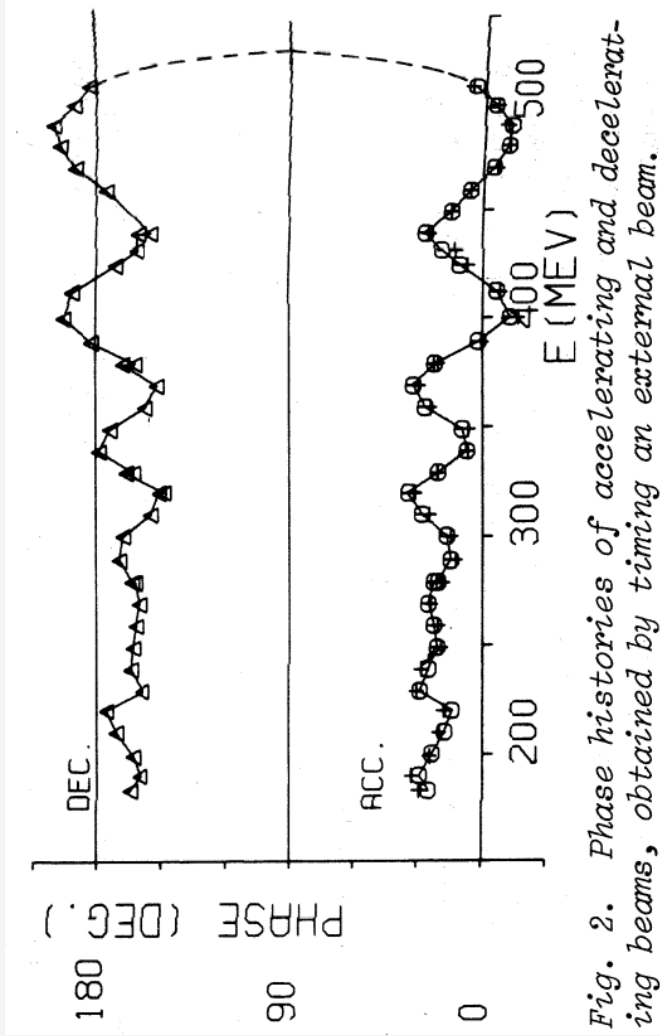


Serpentine Acceleration

Measured by:

M. Craddock, PAC 1977

Simulated using **CYCLOPS**
generated matrices:





Even more serpentine than in EMMA, like a snake

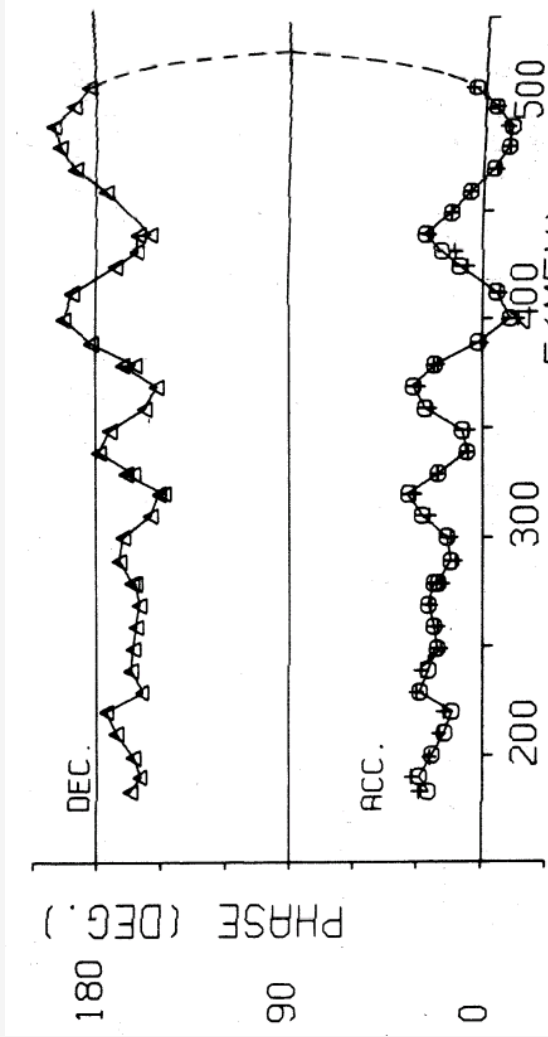
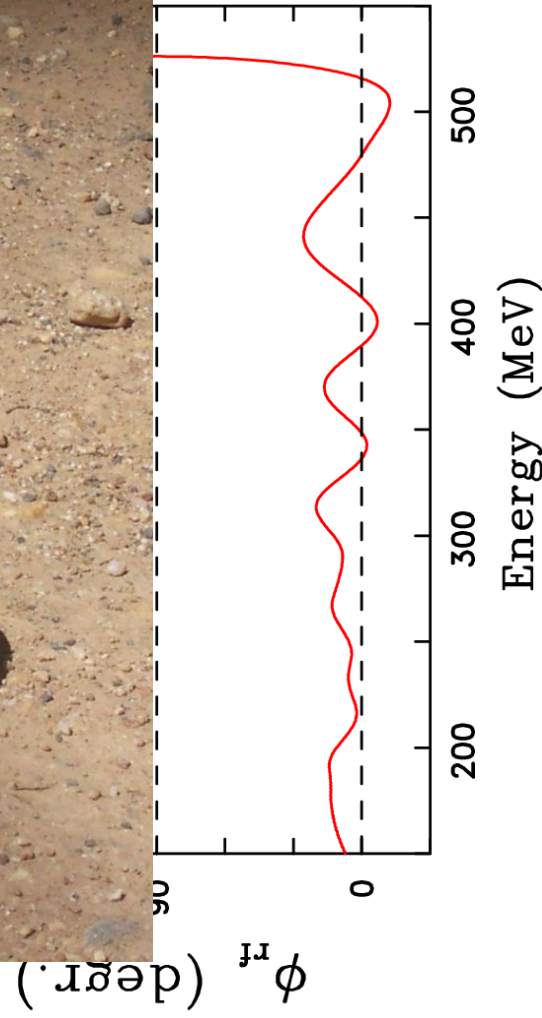


Fig.
ing





**In one word,
CYCLOPS has
sufficient accuracy!**

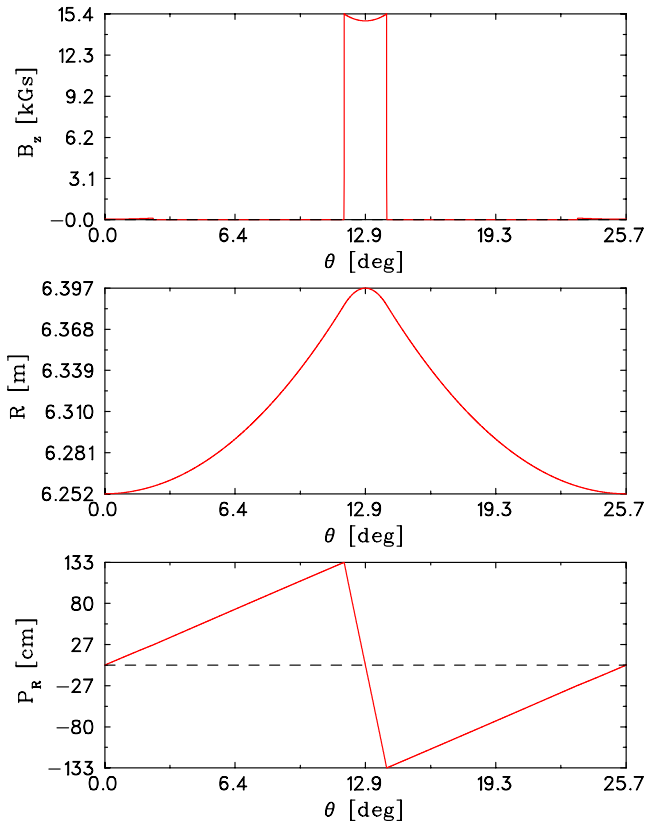


Fig. 1. B_z (vertical) field at injection for nonscaling FFAG lattice showing sharp cutoff of field at end of CF magnet, along with the radius of the injected orbit along the periodic cell and the angle as measured with respect to a normal projection relative to a radial line.

description and are limited to low order in the dynamics. This limitation can be inadequate to fully demonstrate performance including dynamic aperture where strong nonlinearities due to edge fields and other high-order effects appear. This is particularly true for the FFAGs. In the muon FFAGs, for example, the large beam emittances require the inclusion of kinematical (or angle) effects in the Hamiltonian, which implies that codes which fully describe the kinematics are necessary.^{6,7}

The current number of supported design and optimization codes that can adequately describe the complex field and magnet contours for both the scaling and nonscaling FFAG variants is limited. Outside of COSY, present public codes include only the cyclotron code CYCLOPS,⁸ and the field-map code ZGOUBI.^{9,10} The former, which utilizes fields and their geometry expanded in polar coordinates, has limited accuracy in this application primarily due to lack of out-of-plane expansion order, and in handling of edge-field effects; this is particularly true for the case of rapid azimuthal field fall off at magnet edges (as in the FFAG field profile of Fig. 1), an effect not present in cyclotrons. The results and derived performance

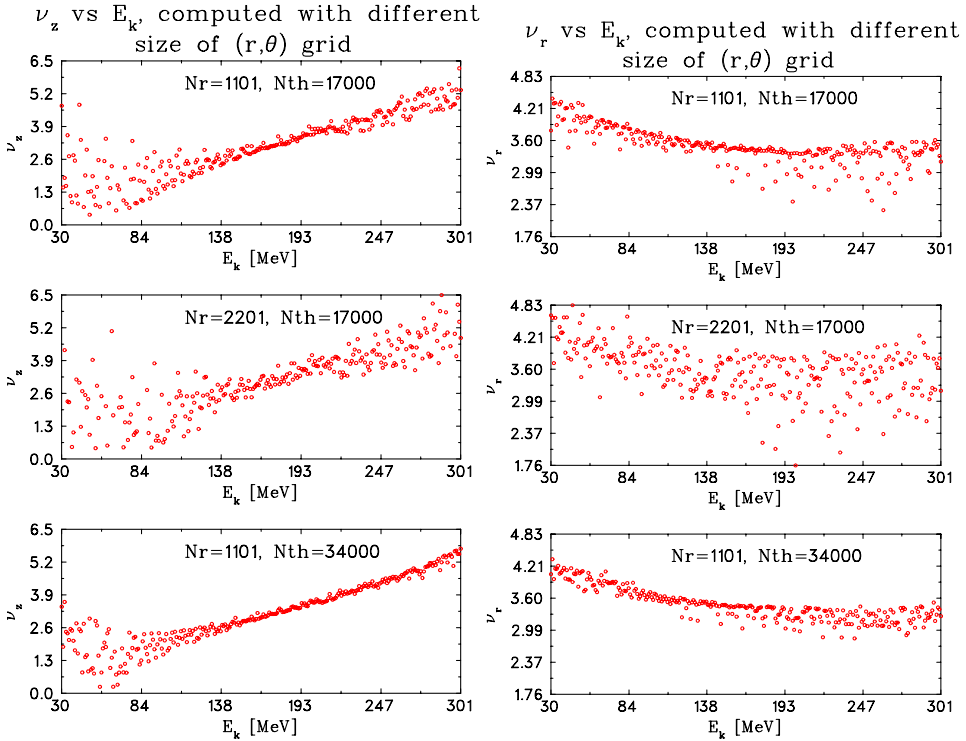


Fig. 2. Radial and azimuthal tunes for a 14-cell, 30–400 MeV nonscaling proton FFAG showing dependence on number of radial (N_r) and azimuthal (N_θ) mesh points used in field calculation.

can be strongly dependent on the integration step size across such an edge with Fig. 2 showing results for different mesh sizes. **Since Cyclops remains a cyclotron code, it does not directly incorporate field data, either calculated or measured, primarily derives only closed orbits and tunes for an FFAG, and has no standard models to handle fringe fields.** (Particle tracking and dynamics require another associated code.) The latter code, ZGOUBI, is presently being used successfully in FFAG development, but requires dedicated effort and expertise to implement an FFAG design, particularly when expressed in terms of the conventional magnetic component definitions. At present, some modern analysis tools for symplectic tracking, global optimization, tuneshifts and chromaticities, and resonance analysis are not as yet available.

In the following an analysis of a 14-cell, linear-field nonscaling 400-MeV FFAG for protons is compared between MAD, ZGOUBI, and CYCLOPS. (In MAD, the simulations were performed at discrete energies based on a derived closed orbit.) The results from MAD reflect a simple hard-edge. Field modeling in Cyclops reflected the hard edge representation, but experienced difficulty in calculating tunes with strong sensitivity to the fineness of mesh size discretization near the edge (Fig. 2). A considerable degree of effort¹¹ was expended in ZGOUBI to effect both the edge

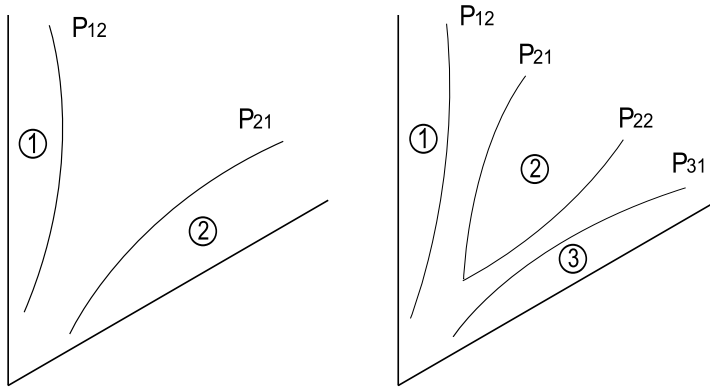


Fig. 6. The curves describing the effective field boundaries of the FFAG magnets in a cell of angle π/n in the two-bend (left) and three-bend (right) case.

where the origin of the coordinate system is at the center of the accelerator. In the vicinity of an edge curve, the fringe field belonging to the magnet bounded by that curve is given by an Enge Function

$$B_y(x, z) = \bar{B} \cdot \frac{1}{1 + \exp(P_i(d/D_i(r)))}$$

where \bar{B} is the main field acting at the point closest to (x, z) on the effective field boundary and P_i is a polynomial. Note that \bar{B} is the sum of the contributions from the individual multipoles. The quantity d is the distance of the point (x, z) to the effective field boundary, and D_i is the aperture of magnet i , which is allowed to vary with radius in polynomial form.

Enge functions provide significant flexibility for the description of most types of realistic field fall-offs by appropriately choosing the coefficients of the polynomial in the exponential function. Thus, fringe field profiles based on other explicit functions are usually not necessary, at least in early stages of design.

Fringe fields of neighboring curves are allowed to overlap. Overall, the fringe field description is very similar to the approach that has been followed very successfully in the study of high-resolution particle spectrographs.

The advantage of this particular field model is that it allows a relatively simple adjustment of the main parameters commonly studied in the design of FFAG magnets while providing a fully Maxwellian and realistic field description. Specifically, the radial field variation appearing in $P_{B,i}(r)$ affects both the horizontal and vertical focusing for quadrupole and higher fields and only horizontal focusing for dipole, and the edge curves $\vec{P}_{ij}(t)$ affect both horizontal and vertical focusing. The Enge fall off is well known to represent realistic field profiles which can be adjusted to accurately describe most magnets and can even approximate a rapid, hard edge fall-off which is useful for comparison with codes without fringing fields.

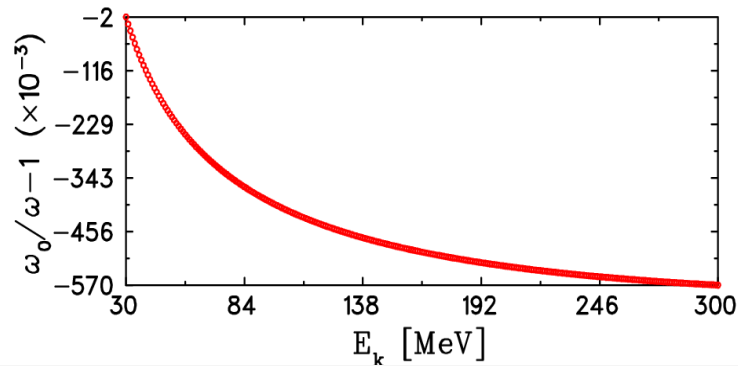
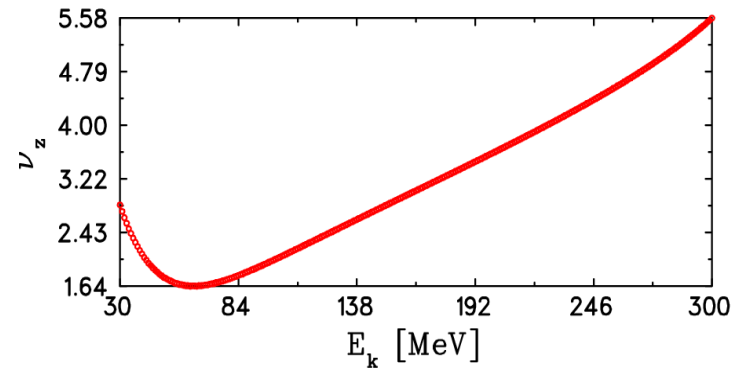
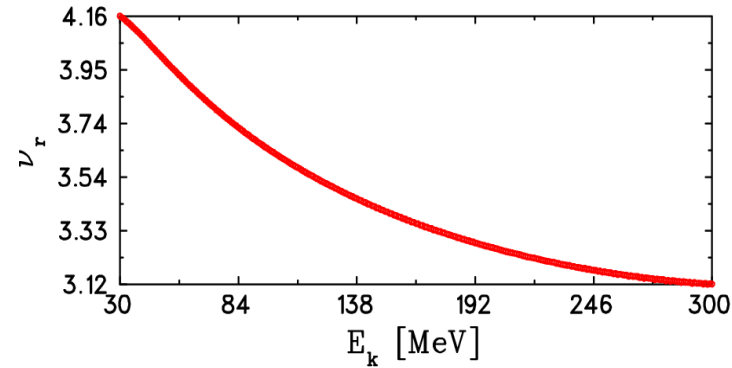


Discontinuous Sector Fields

- CYCLOPS needs fields on a polar grid; none of them are artificially generated.
- Discontinuous sector fields, i.e. hard-edge fields, are artificially generated; NOT physical.
- **Can COSY handle discontinuous fields? NO!** It just has built-in fringe fields that roll off according to some analytic function.
- CYCLOPS works nicely too with the Enge-function modelled fringe fields.

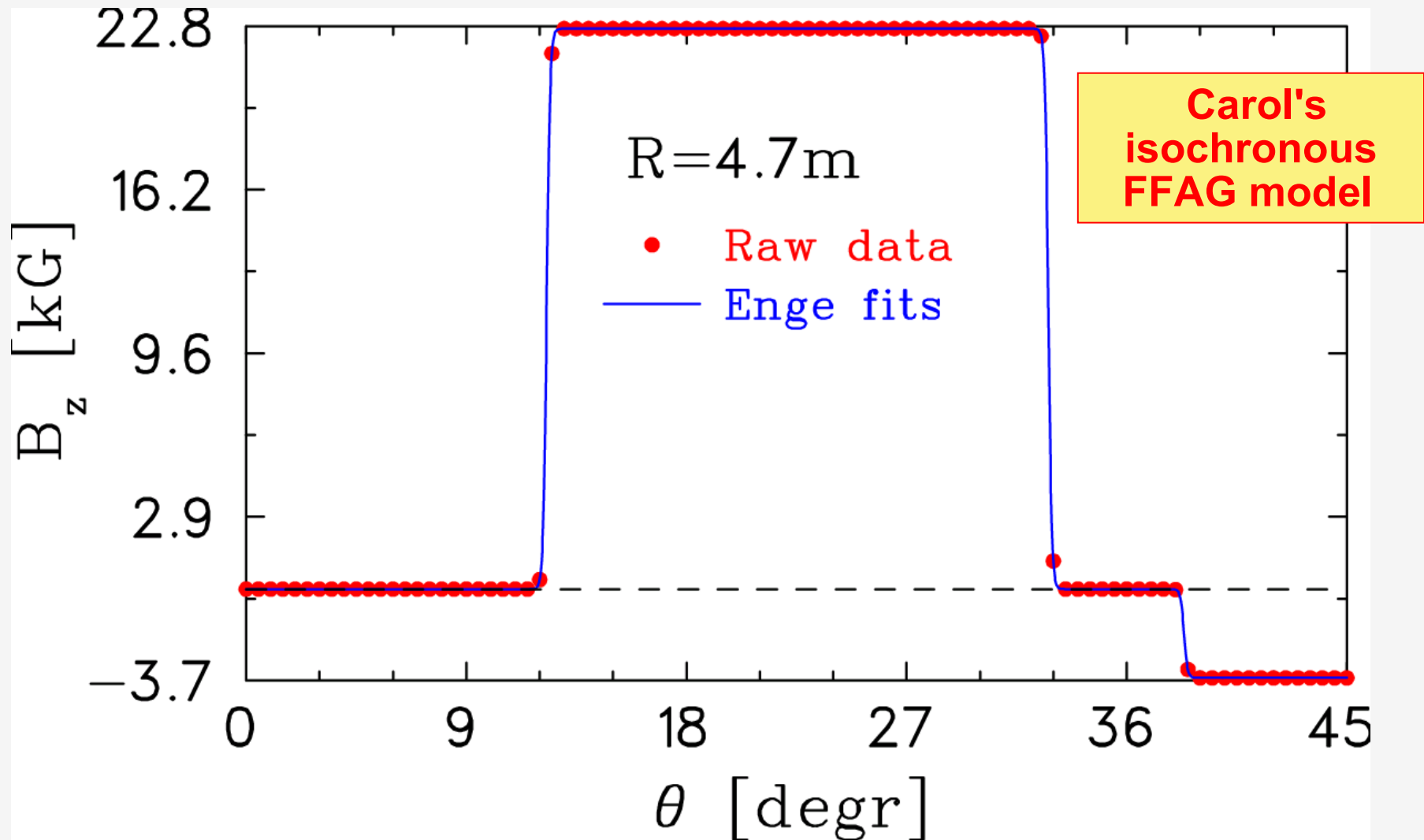


CYCLOPS does give completely smooth results!



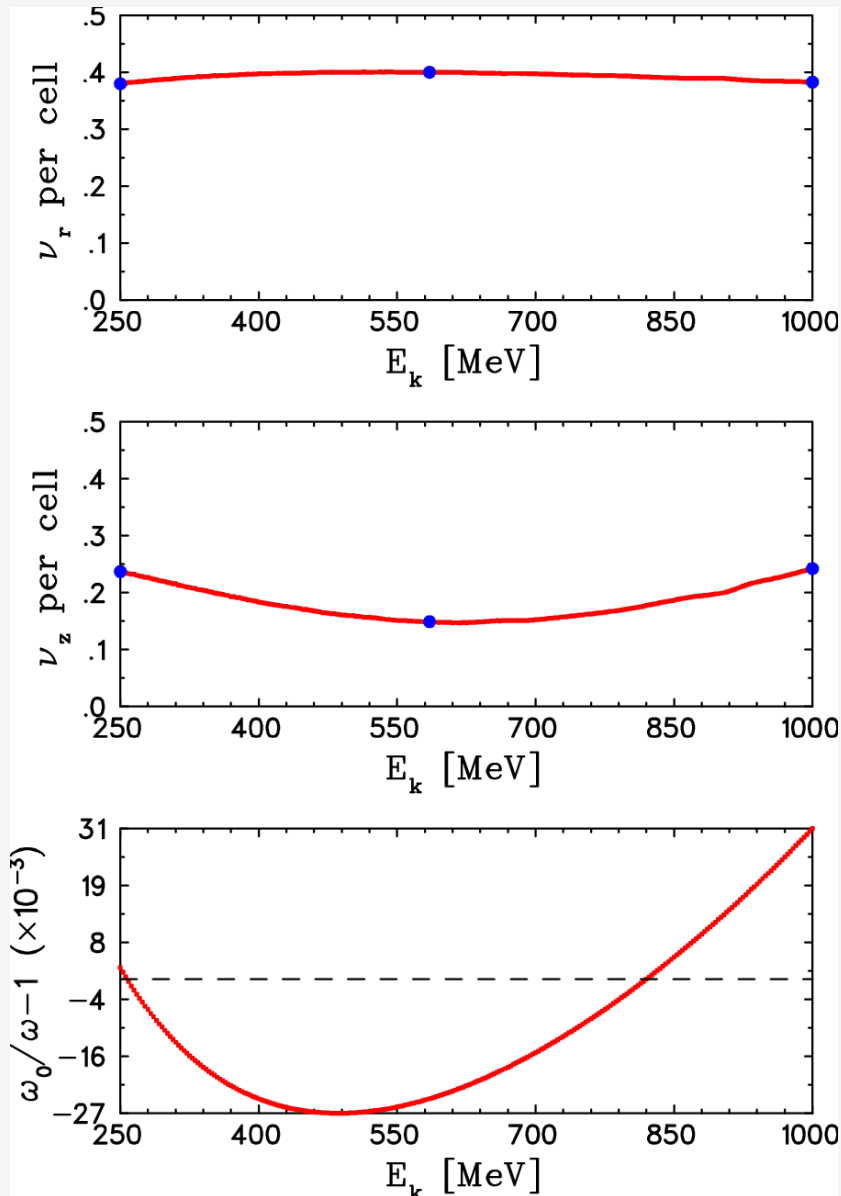


Enge-Function Fringe Fields





CYCLOPS gives completely smooth results!

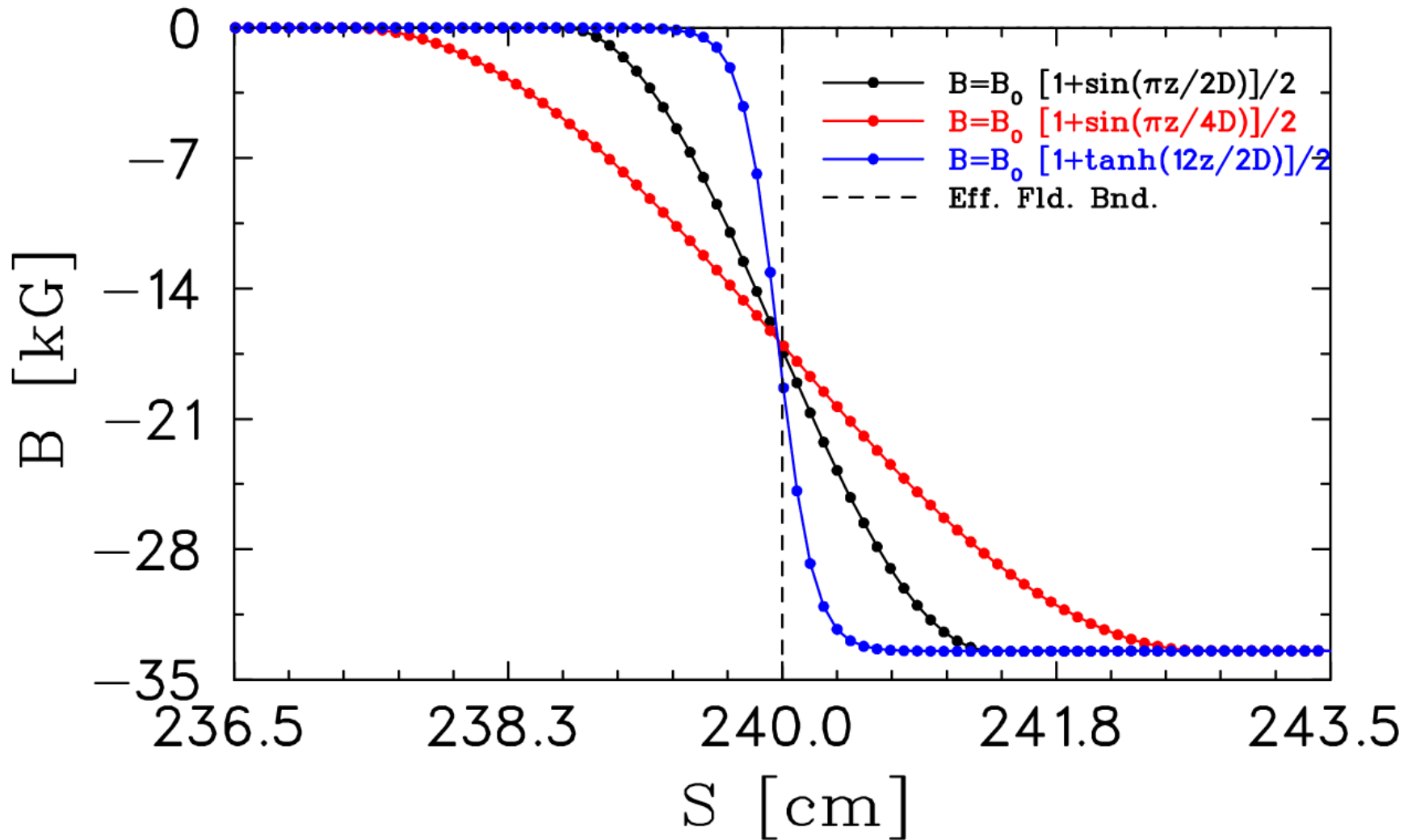


But, for which
COSY had **only**
been able to
provide values
at **three** discrete
energies.
-- Craddock & Rao,
IPAC 2010



Tune is almost f.f. shape independent.

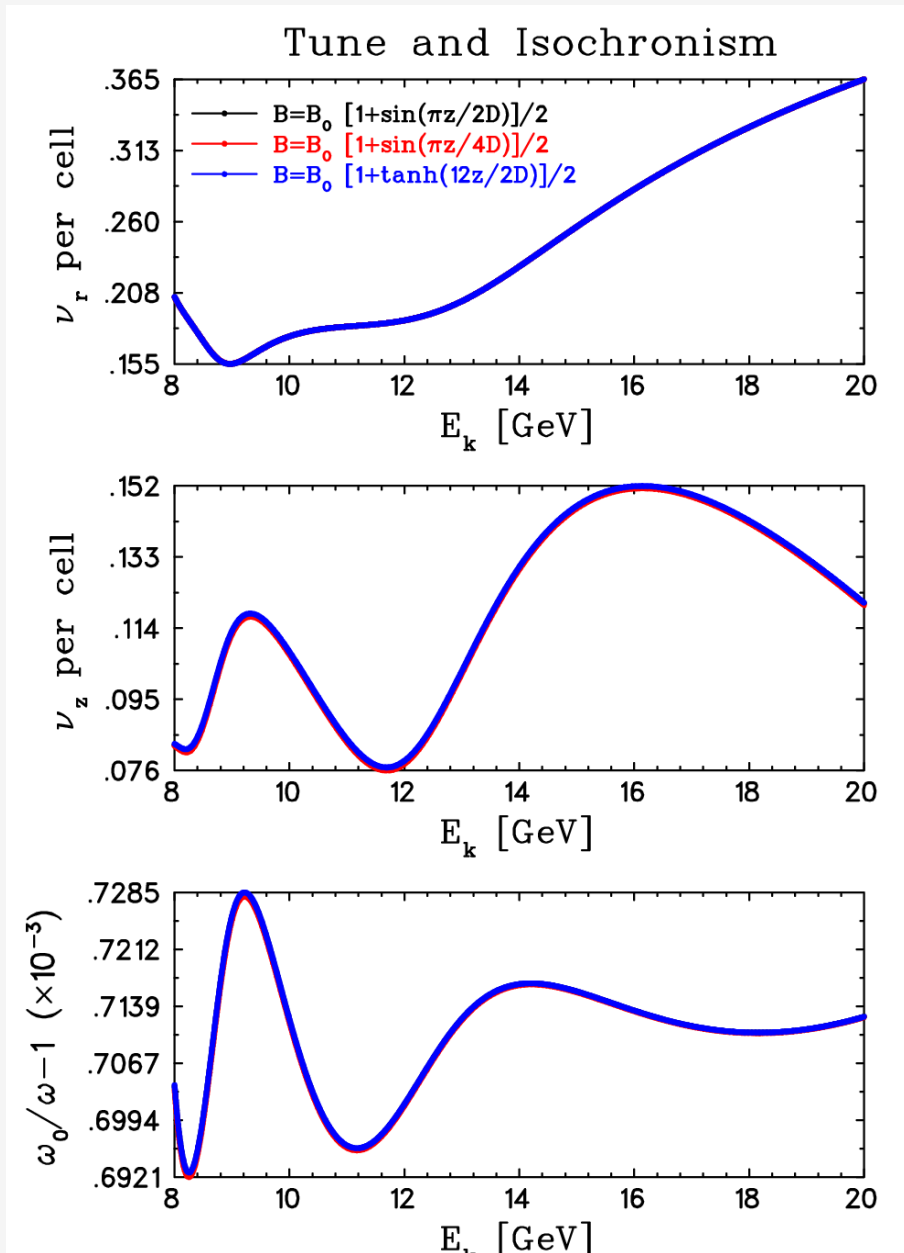
Fringe Field Shape





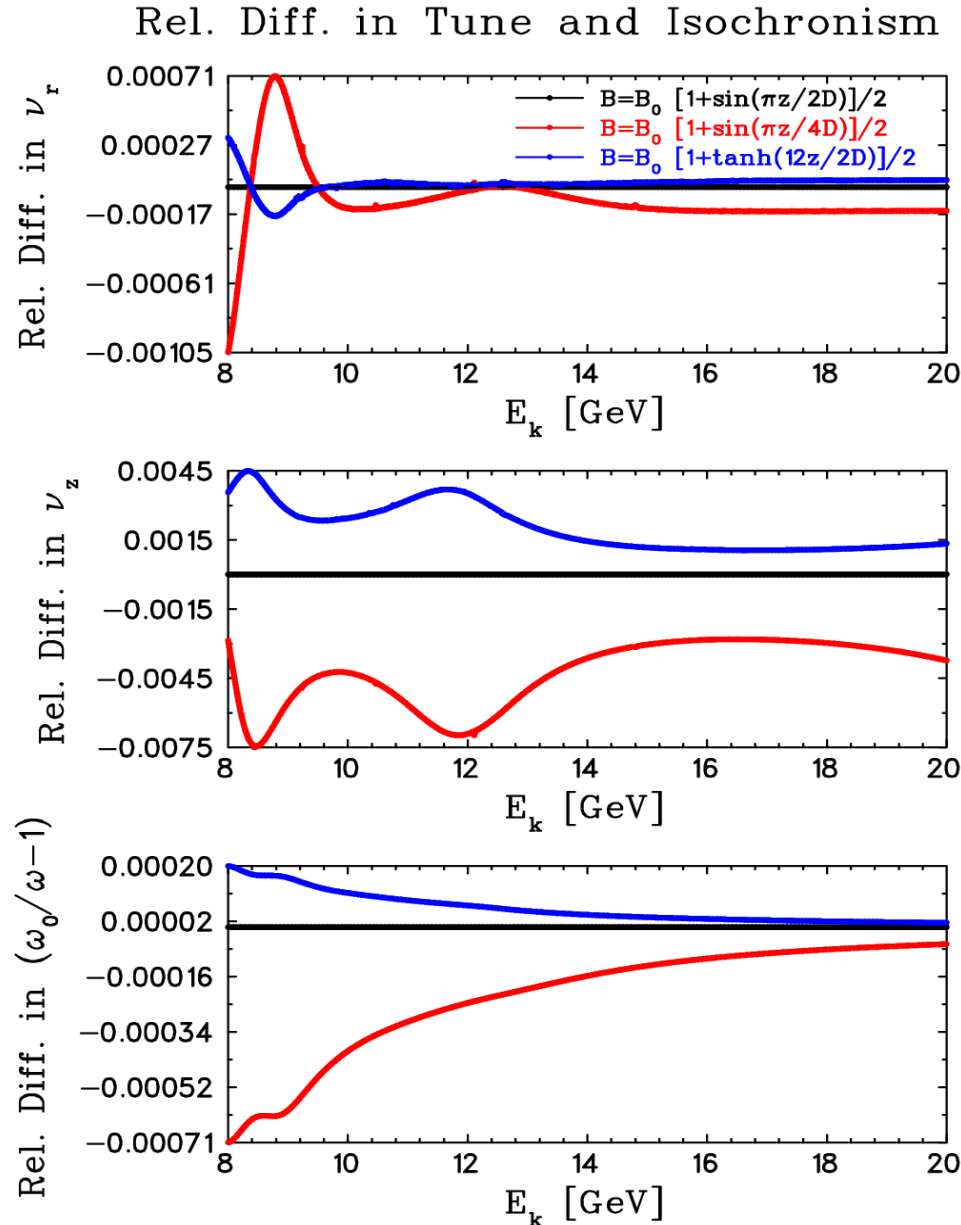
Tune is almost f.f. shape independent.

Rees's IFFAG



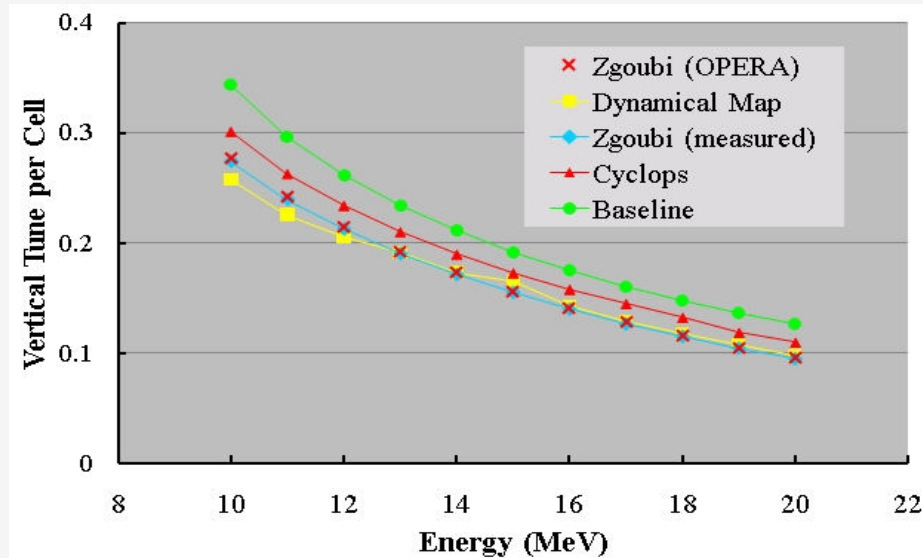
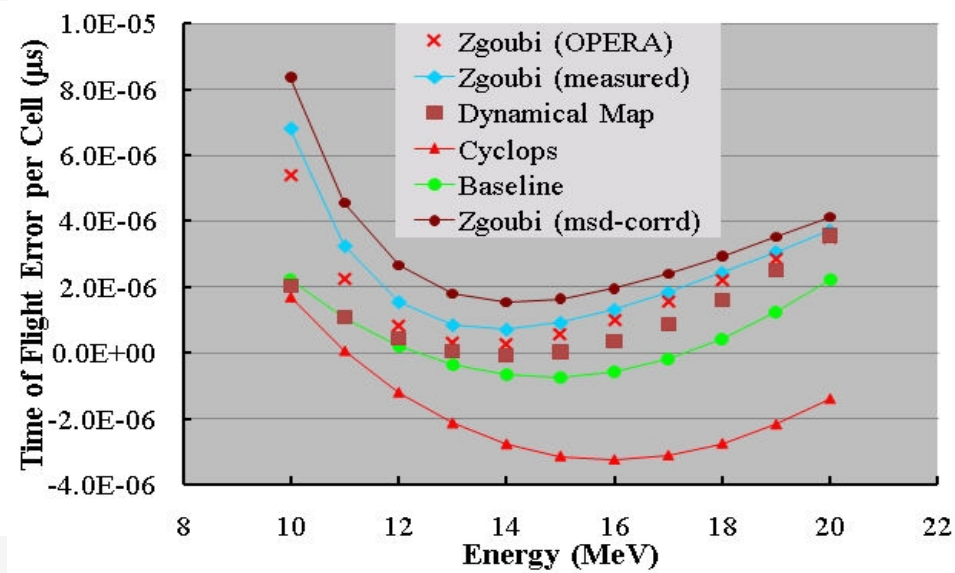
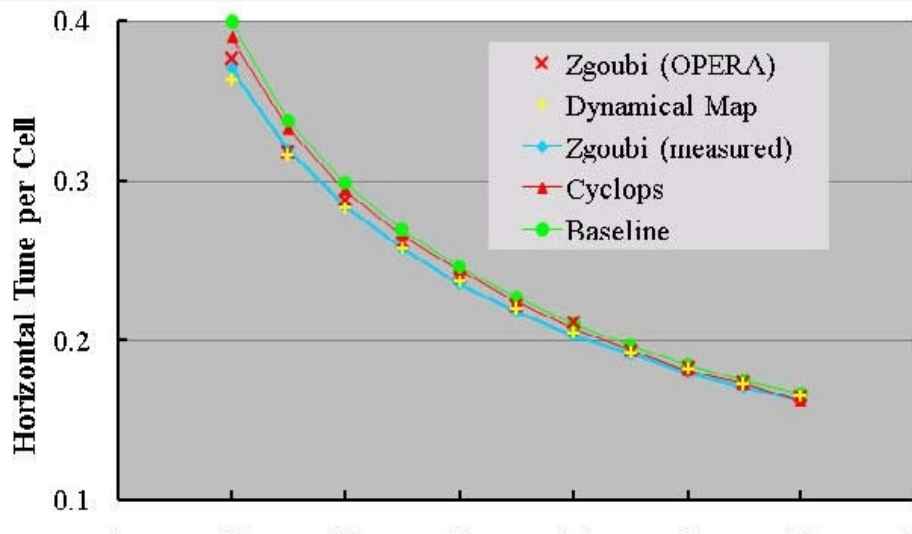


Tune is almost f.f. shape independent.





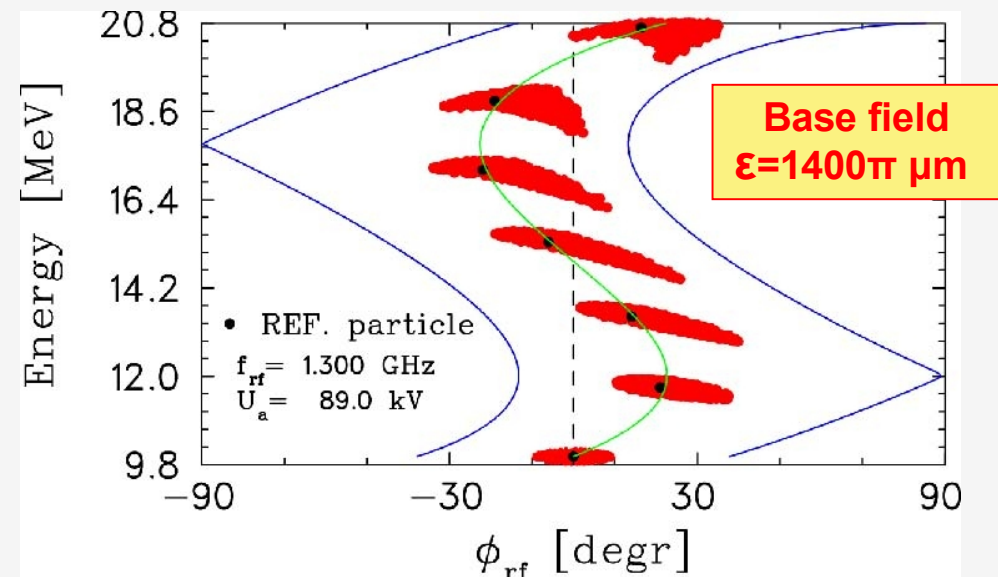
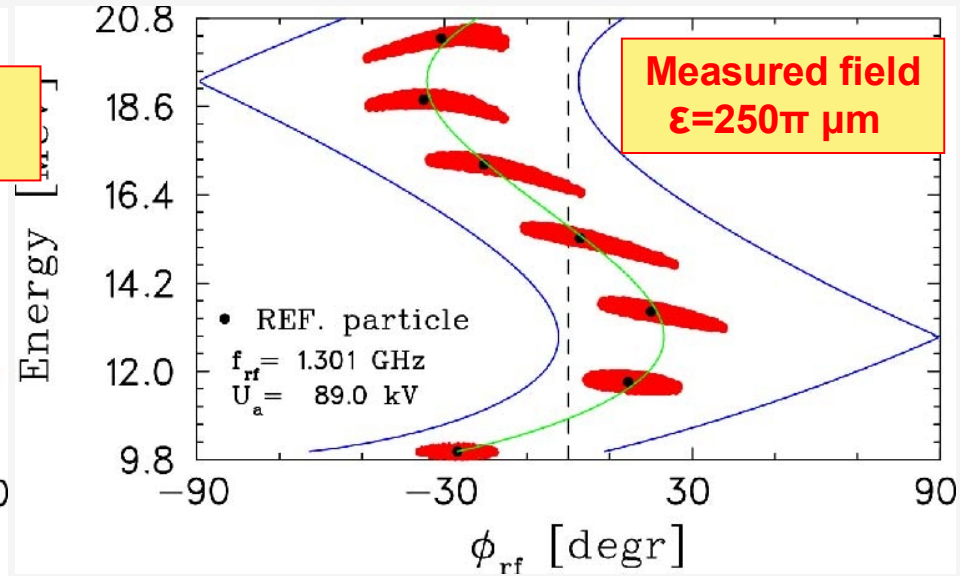
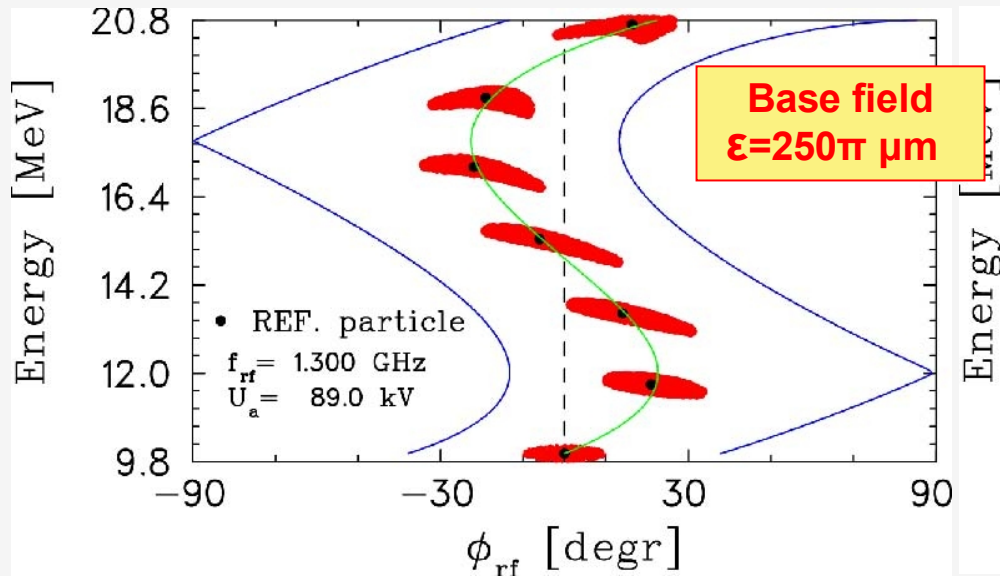
EMMA: Tune & Orbit Time



Craddock & Rao,
IPAC 2010



EMMA: Accelerated Orbit simulated using GOBLIN, sister of CYCLOPS



Craddock & Rao,
IPAC 2010



Conclusions

- With great success, **CYCLOPS** was used to design the world's largest linear dimension's cyclotron **with sufficient accuracy.**
- **CYCLOPS** works nicely with any physical magnetic fields given on the polar grids.
- **CYCLOPS** **works nicely too with Enge-function modelled fringe fields.**
- **CYCLOPS** is very fast and efficient. In 1973, computing power was many orders of magnitude less than today, and yet we designed a cyclotron. If you transport **COSY-infinity** or any of today's simulation codes, to the early 70s, it would have been useless. Every shimming required finding and analyzing 700 orbits. This took about 2 hours on the IBM360. It would have taken months with today's codes. **Today, CYCLOPS takes about 15 milliseconds per orbit.**



Thank you for your attention.

**4004 Wesbrook Mall
Vancouver, B.C. Canada V6T 2A3
Tel: 604 222-1047 Fax: 604 222-1074
www.triumf.ca**

EMMA: Comparison between Hard-Edge Baseline Field and Measured Field

Y.-N. Rao
Mar.24, 2010

1 Layout and Dimensions

Figure 1 shows the sketches of the layout of a single cell, and the dimensions.

2 Fields on the Polar Grids

Figure 2 shows the field strength on the polar grid (r,θ) , generated for the CYCLOPS run.

3 Equilibrium Orbit Properties

Figure 3 shows the CYCLOPS calculated tunes and isochronism vs. energy.

Figure 4 shows the orbital time vs. energy.

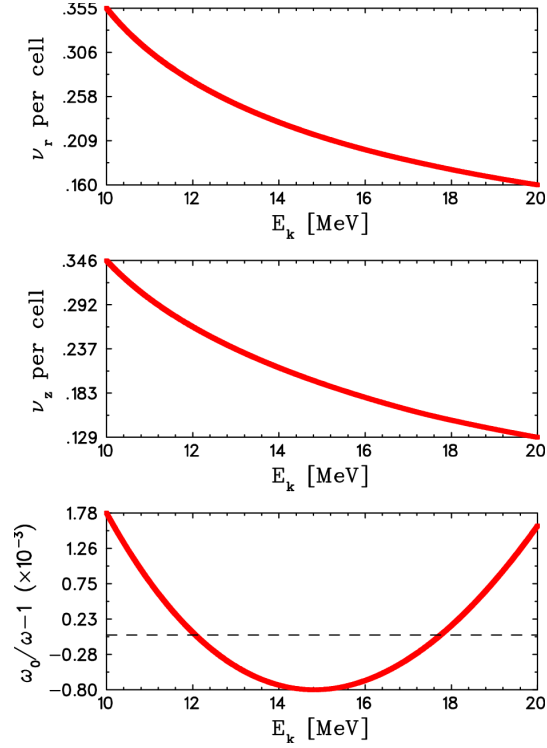
Figure 5 shows the field value, r and p_r on the equilibrium orbits of various energies.

4 Accelerated Orbits

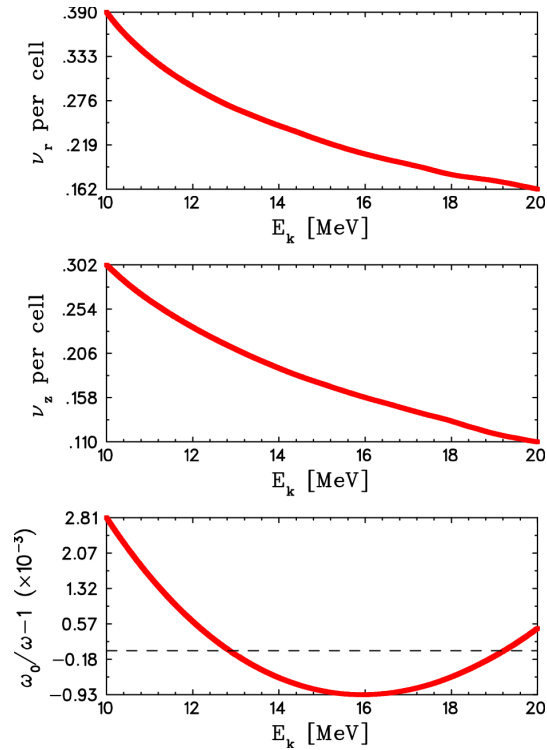
Figures 6-11 show the longitudinal phase space trajectory, simulated using GOBLIN and calculated using the phase-energy equation.

5 Conclusion

Does the measured field result in the same as the hard-edge baseline field predicted? No.

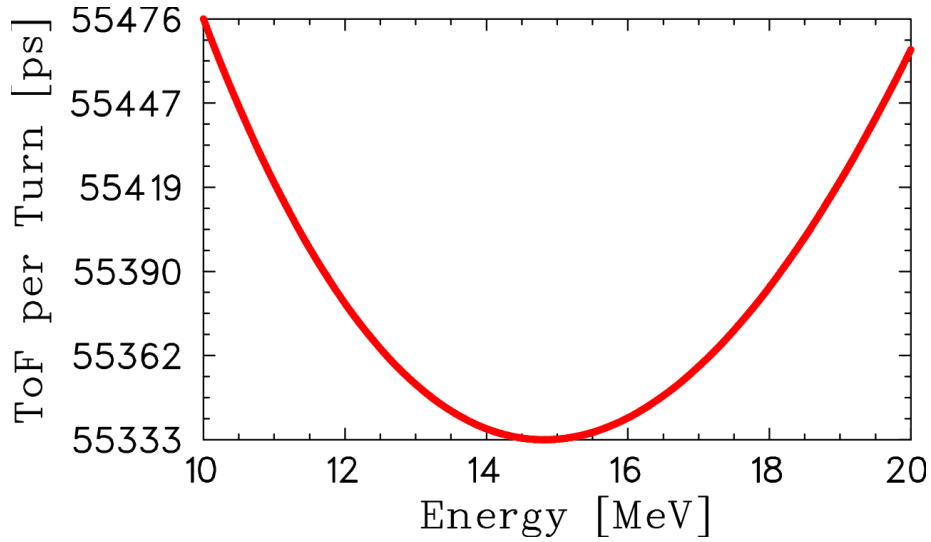


(a). Results from the hard-edge baseline field, where $f_{rf}=1.300172495$ GHz, harmonic number=72.

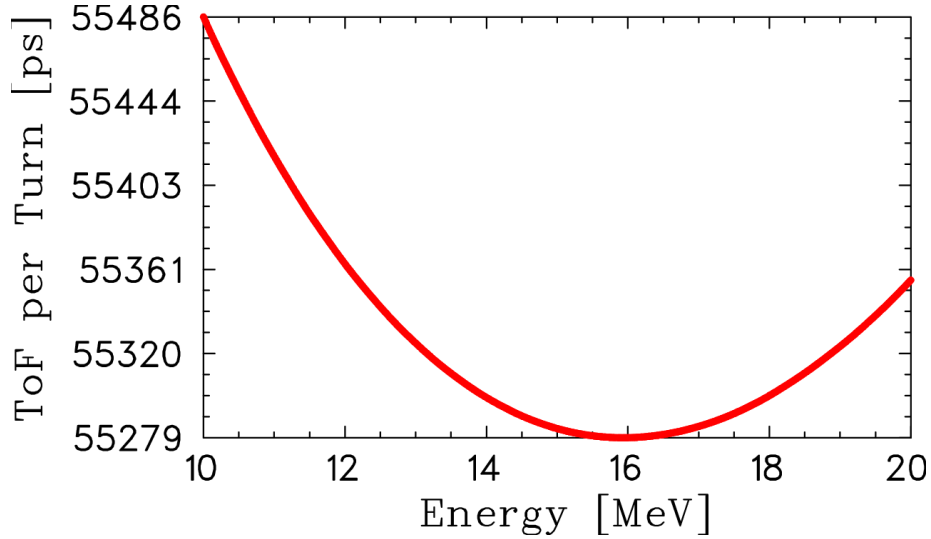


(b). Results from the measured field, where $f_{rf}=1.301280998$ GHz, harmonic number=72.

Figure 3: CYCLOPS calculated tunes and isochronism vs. energy.

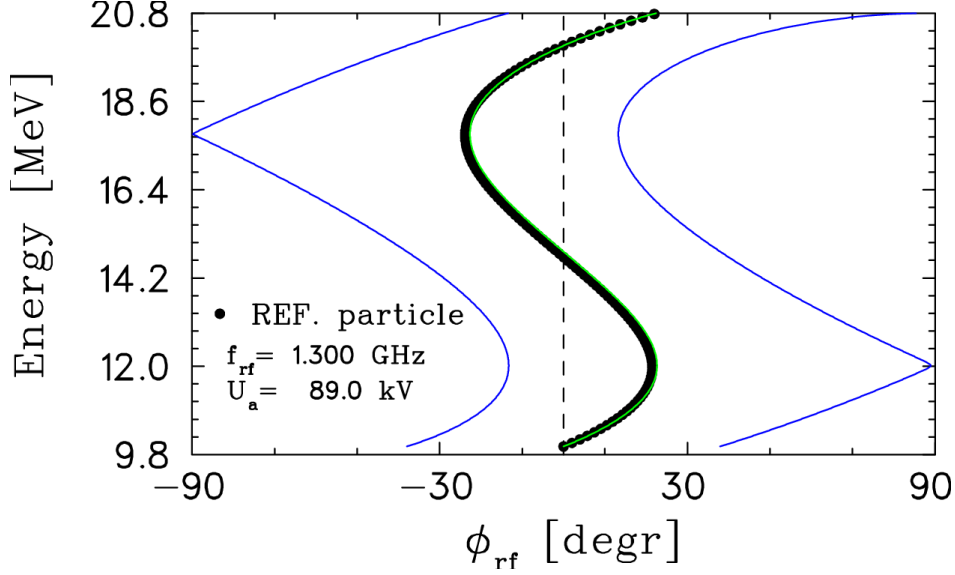


(a). ToF from the hard-edge baseline field, where the minimum occurs at ~ 14.810 MeV.

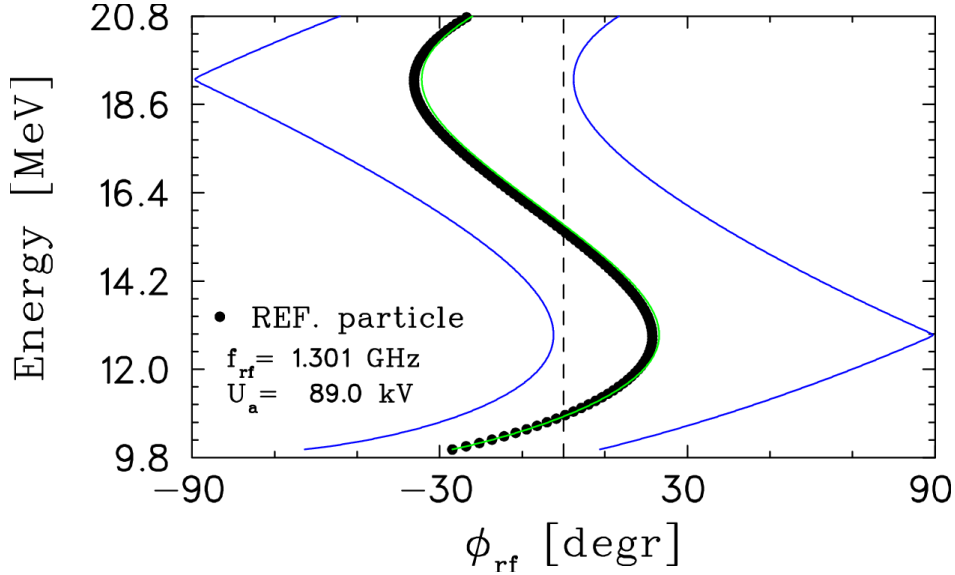


(b). ToF from the measured field, where the minimum occurs at ~ 15.930 MeV.

Figure 4: CYCLOPS *calculated orbital ToF per turn vs. energy.*

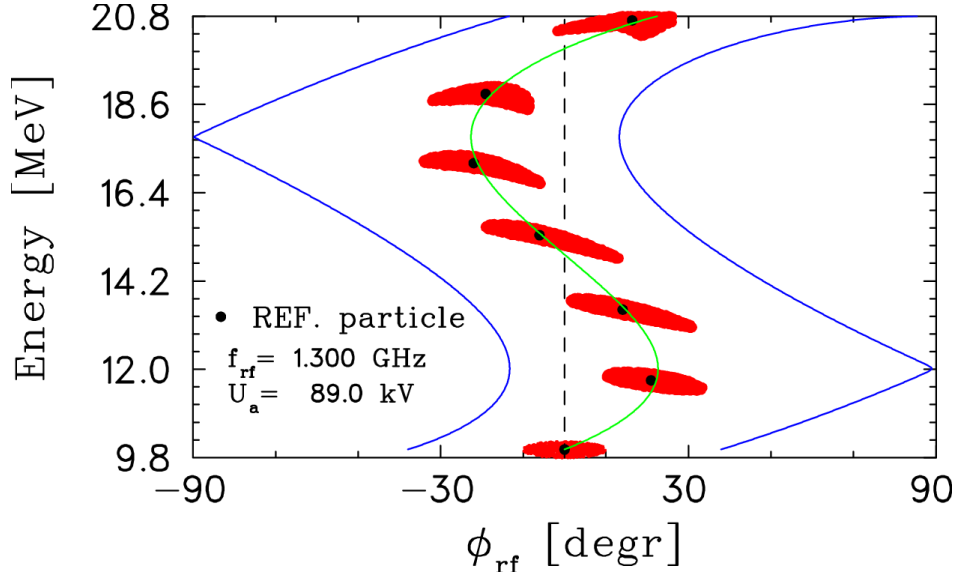


(a). Result from the hard-edge baseline field, where $f_{rf} = 1.300172495$ GHz.

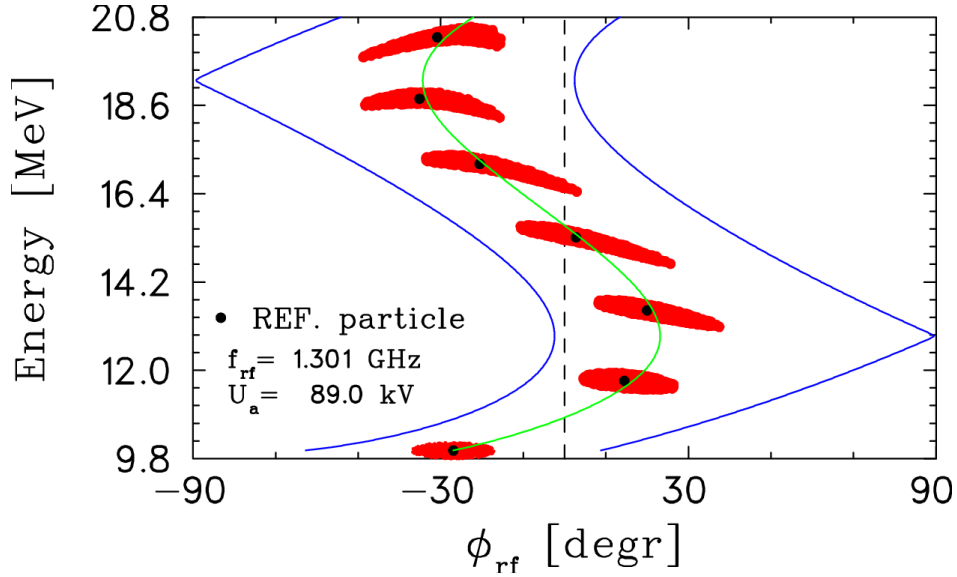


(b). Result from the measured field, where $f_{rf} = 1.301280998$ GHz.

Figure 6: Longitudinal phase space trajectory at each crossing of rf cavities, simulated using GOBLIN (black dots) and calculated using the phase-energy equation (blue and green curves) $\sin \phi_2 - \sin \phi_1 = \frac{2\pi h(1+\epsilon)}{qU_a} \int_{E_1}^{E_2} \left(\frac{\omega_0}{\omega} - 1\right) dE$. There were 21 rf cavities assumed and evenly populated, with an amplitude of 89 kV for each. The starting phases for the 2 blue curves were adjusted manually such that they reached $\pm 90^\circ$ at maximum; while the starting phase for the green curve was the middle value between these 2 blue curves. For the GOBLIN simulations, the 21 cavities were initially phased in terms of the ToF of reference particle, and the reference particle started on a corresponding static equilibrium orbit radially. As a result, the reference particle is almost riding on the green curve all the way. Note that the rf frequency values are different by ~ 1.1 MHz.

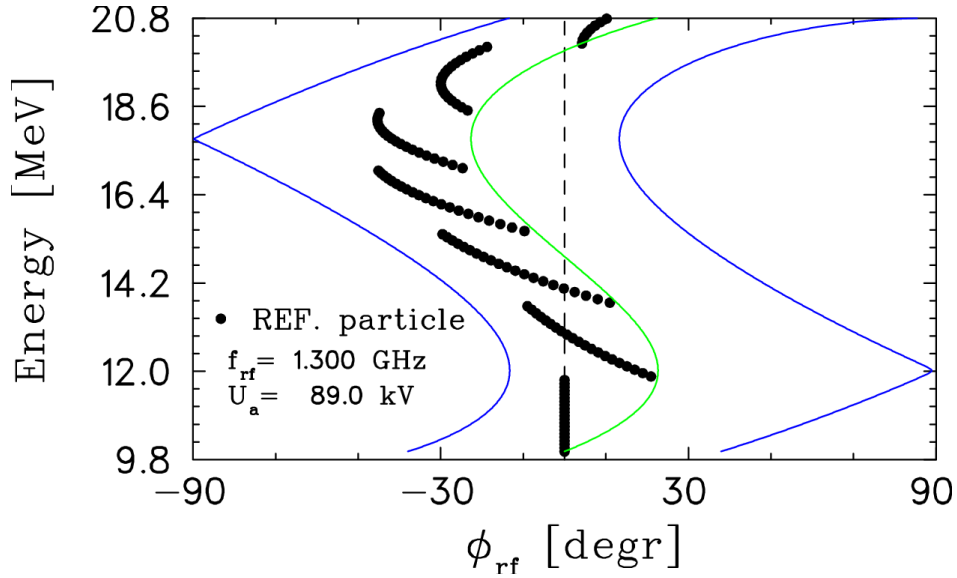


(a). Result from the baseline field.

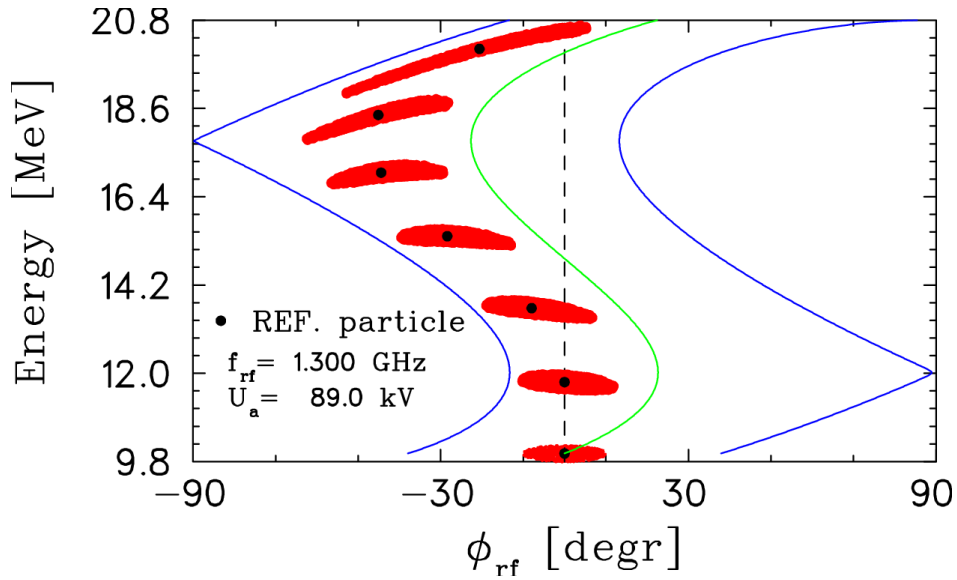


(b). Result from the measured field.

Figure 7: GOBLIN simulations of acceleration for a beam bunch. The 1st ellipse is plotted with the initial conditions, before passing through any cavities, but the 2nd ellipse is plotted after 20 cavity passages, and the 3rd, 4th, 5th, 6th and 7th ellipses are made at the same azimuth as the 2nd ellipse but after 41, 62, 83, 104 and 125 cavity passages respectively. The initial conditions of the bunch are: phase width of 20° , energy spread of $(10 \pm 0.2) \text{ MeV}$, and radial emittance of $250 \pi \text{ mm-mrad}$ (normalized). All the other parameters are completely the same as in Fig.6.

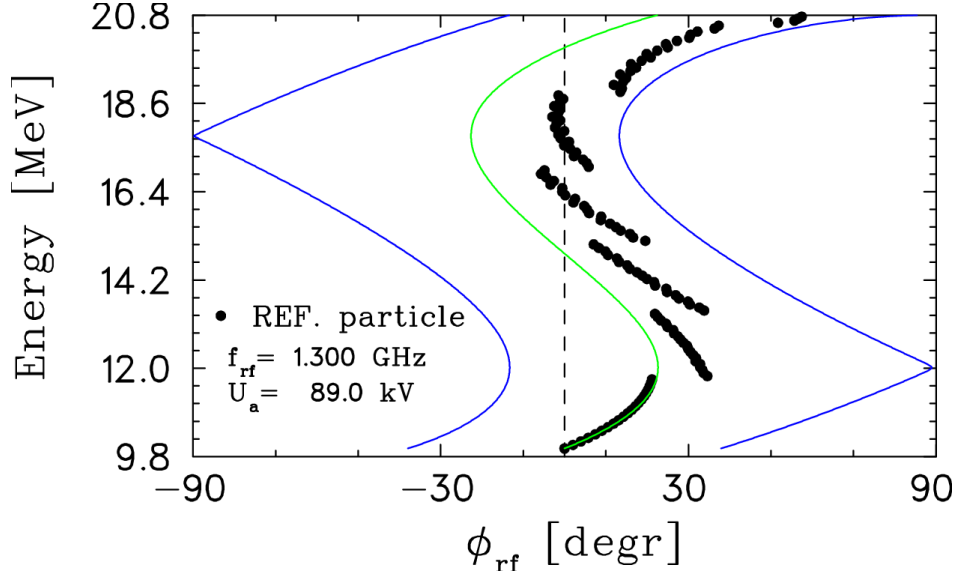


(a). Reference particle at each crossing of rf cavities.

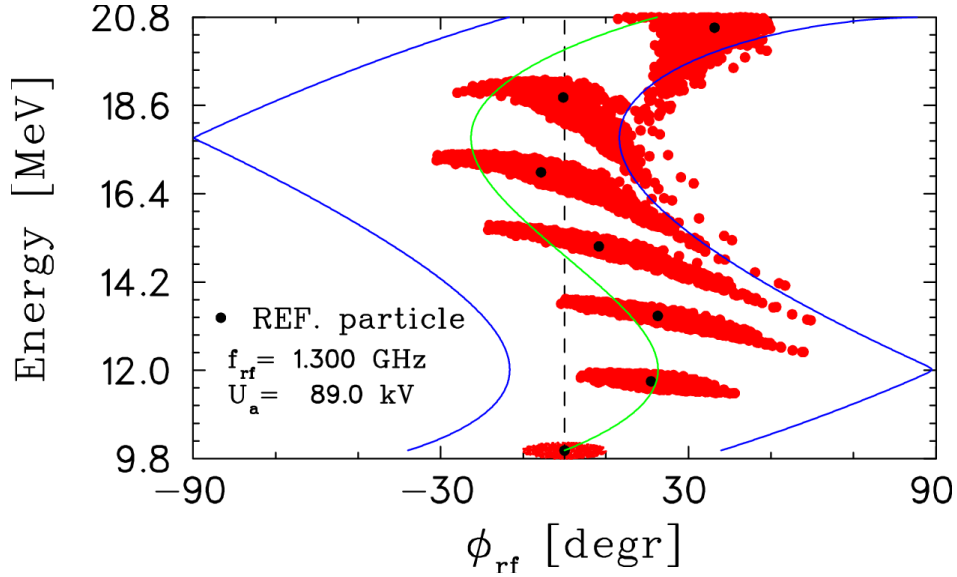


(b). Bunch at start and after 20, 41, 62, 83, 104 and 125 cavity passages respectively.

Figure 8: *Results of simulation performed with the hard-edge baseline field. Except that the initial phases of the 21 cavities are changed and assumed identical, parameters used are completely the same as in the Figs.6 and 7. Comparing with Figs.6 and 7, one can see that improper initial phases of cavities lead to elongation of bunch.*

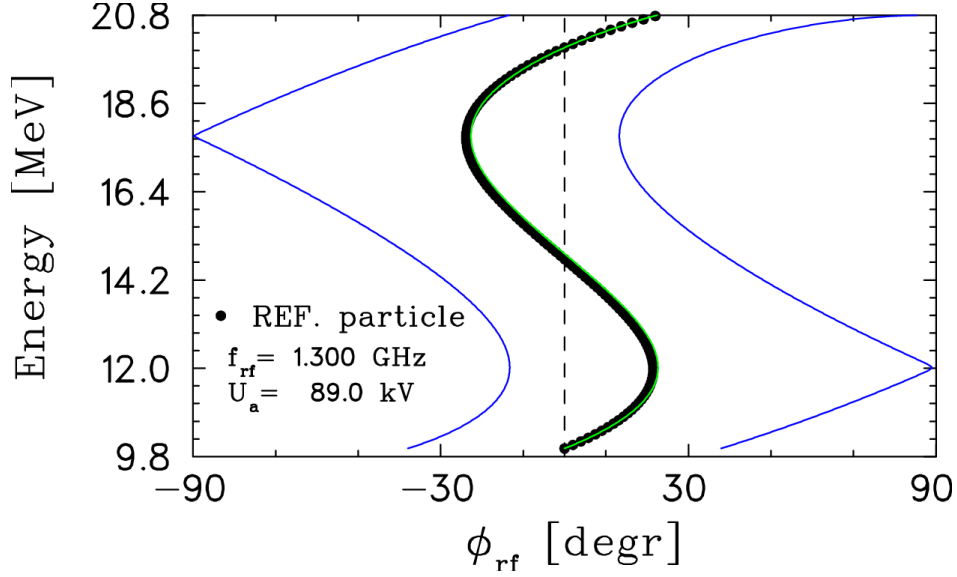


(a). Reference particle at each crossing of rf cavities.

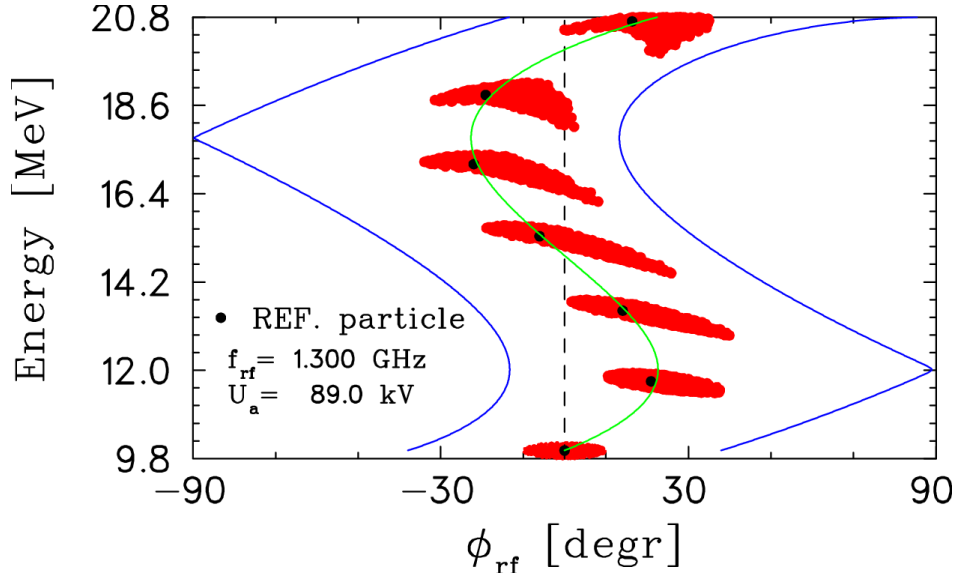


(b). Bunch at start and after 20, 41, 62, 83, 104 and 125 cavity passages respectively.

Figure 9: Results of simulation performed with the hard-edge baseline field. Except that the initial values of r and p_r are changed deliberately such that particles are off centered radially, parameters used are completely the same as in the Figs.6 and 7. Comparing with Figs.6 and 7, one can see that off-center of initial beam causes a distortion of bunch, and even, some particles cannot get to the extraction energy of 20 MeV.

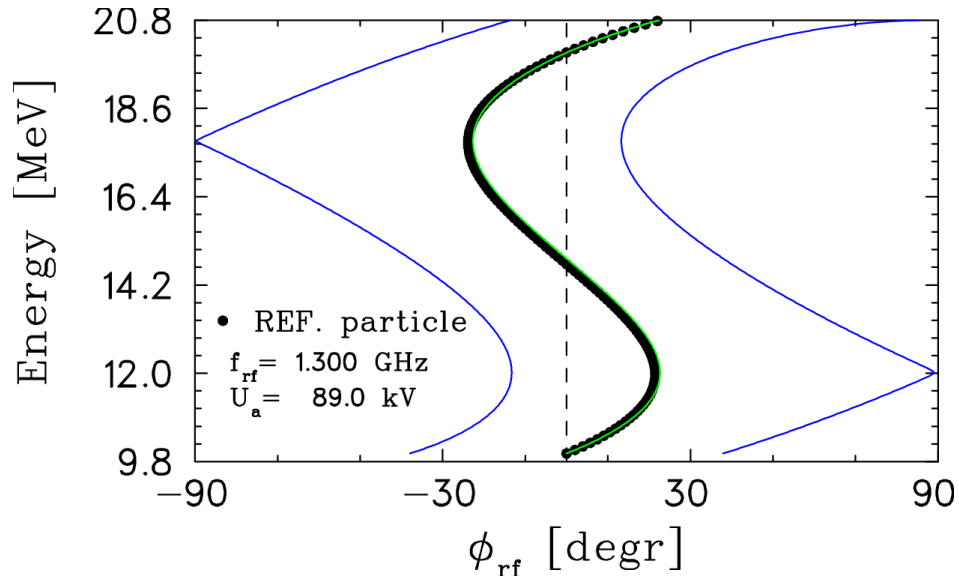


(a). Reference particle at each crossing of rf cavities.

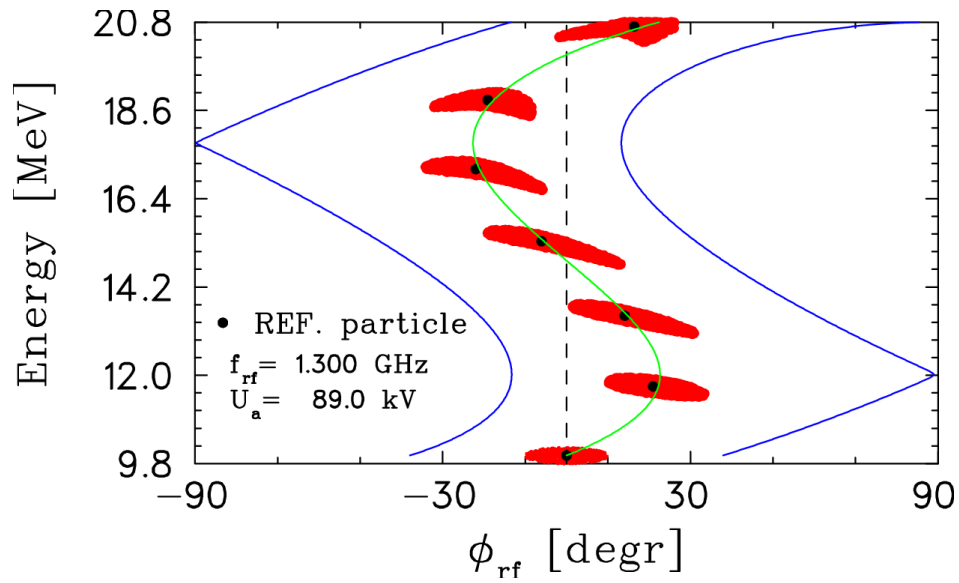


(b). Bunch at start and after 20, 41, 62, 83, 104 and 125 cavity passages respectively.

Figure 10: *Results of simulation performed with the hard-edge baseline field. Except that the initial radial emittance is increased from 250 to $1400\pi\text{mm-mrad}$ (normalized), parameters used are completely the same as in the Figs.6 and 7 (or Fig.11). Comparing with Fig.11, one can see that the larger the radial emittance, the more significant the ellipses distortion. This is arisen from the radial amplitude dependence of the orbital ToF.*



(a). Reference particle at each crossing of rf cavities.



(b). Bunch at start and after 20, 41, 62, 83, 104 and 125 cavity passages respectively.

Figure 11: Same as those shown in Figs.6 and 7. The radial emittance at start is $250\pi\text{mm-mrad}$ (normalized).

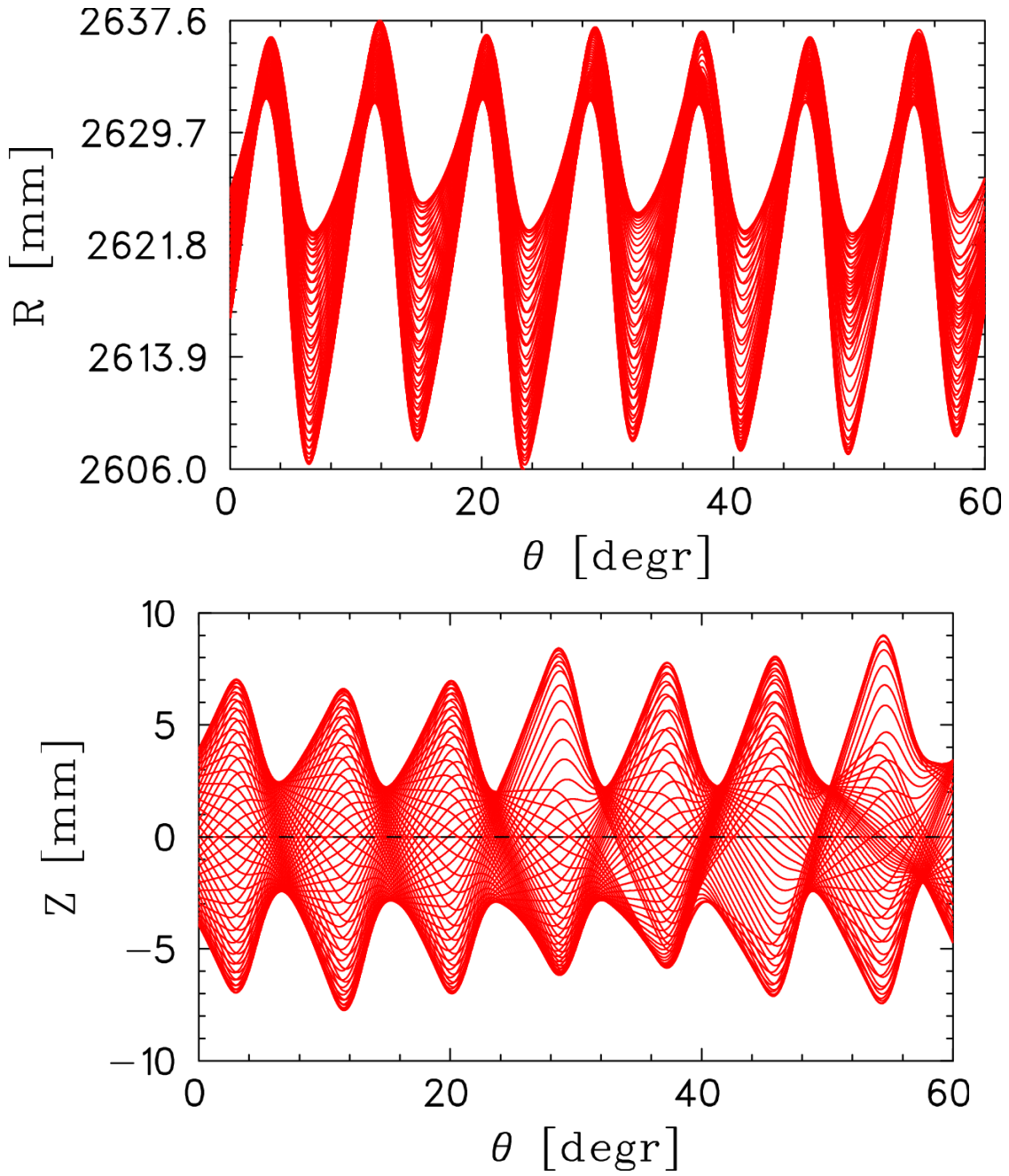


Figure 2: R and Z vs azimuth on the first turn (here only plots up to 60°), where $f_{rf}=1.249762681$ GHz and the first-pass rf phase angle of reference particle is -42.7° for every cavity.